CHAPTER 9

Modeling Water Temperature in King County's Agricultural Drainage Watercourses

9.1 Introduction to Water Temperature Prediction (Goal 8)

Water temperature is critical to the chemical and biological processes that define the health of aquatic environments (Brown 1969, USEPA 1997). Elevated temperatures negatively affect salmonid growth rate, metabolism, and disease resistance, as well as the timing of adult migrations, fry emergence and smoltification (NOAA Fisheries 2004). Temperature limits the maximum concentration of oxygen that can remain dissolved in water and available to aquatic organisms. Water temperature has been identified as an important factor limiting salmonid rearing habitat, changing migration timing, and contributing to the decline in salmon population in streams throughout the Pacific Northwest including in the Puget Lowlands and King County (Oregon Fish and Wildlife 1990; Poole et al. 2001; USEPA 2001; Hodgson and Quinn 2002).

Chinook salmon prefer water temperatures between 12 and 14°C with approximately 50% mortality occurring at 26.2 °C (Meehan 1991). The Washington State Department of Ecology and the USEPA recently revised temperature requirements for salmonid habitat in the State as a function of life stage. Current WAC requirements specify 13-17.5°C depending on whether the stream supports salmon spawning, rearing, or migration activities (Ecology 2007).

Most lowland waters that support salmonid rearing, spawning, and migration will be designated under Class A protection. Few water bodies will be designated under Class B protection, which requires a single daily maximum of not more than 21°C and is aimed at protecting salmonid rearing and migration but not necessarily spawning (EPA 2002). Water quality standards are undergoing revision after EPA's review of field and laboratory studies of chronic sub-lethal and lethal temperature effects on fish (EPA 2002). A small, single daily fluctuation beyond a defined daily maximum temperature was found not to be biologically meaningful (EPA 2002). A metric that is overly averaged, such as the seven day average of daily mean temperatures, could mask regularly occurring large diurnal temperature variations out of healthy range (EPA 2002). The seven day average of daily maximum temperatures is the metric identified as the most useful in providing full protection for the individual life-history stages of key species (EPA 2002). For salmon and trout migration and non-core juvenile rearing in the lower part of river basins the proposed seven day average of daily maximum temperature is 18 °C (EPA 2002).

Bormann (2000) lists 45 environmental and physical factors influencing stream water temperature. Among these factors are weather conditions such as air temperature, relative humidity, and wind speed, stream site physical characteristics such as stream width, depth and roughness, and the presence of shading vegetation and topography (Brown 1969, Beschta and Weatherred 1984, Bartholow 1991, Brown and Barnwell1987, Edinger et al. 1968 and Johnson, 2004). Controversy exists regarding the relative importance of riparian vegetation in moderating

stream temperatures. It has been argued that solar radiation is the dominant factor influencing stream temperatures and that the shade of riparian vegetation can significantly reduce stream warming (Brown 1969, Beschta 1997, Theurer et al. 1984, and Chen et al. 1997). Despite a large number of studies there is no consensus on the importance of shade in determining water temperature. Some believe air temperature is primarily responsible for driving stream temperatures and that solar radiation and riparian shade are not significant (Larson and Larson 1996, Larson and Larson 1997, Sullivan et al. 1990, Zwieniecki and Newton 1999). Unlike the influence of ambient weather conditions, riparian vegetation and channel dimensions are uniquely manageable watercourse characteristics. If these characteristics are important to stream temperature, their influence should be determined to identify and prevent anthropogenic temperature increase.

Low gradient agricultural watercourses in King County serve as rearing habitat for ESA-listed salmonids and play a critical role in draining flood waters from agricultural lands. To facilitate drainage, these watercourses have been routinely excavated to remove accumulated sediment and watercourse vegetation. Riparian vegetation is typically partially or completely removed on one bank in the course of drainage watercourse maintenance. Mitigation practices are required in an effort to repair any ecological damage caused by maintenance. The effectiveness of currently required mitigation plantings, and the vegetation type and minimum planting density necessary to protect water temperature are not known. The objective of this study is to identify the impacts of maintenance and mitigation on water temperature.

In addition to protecting water from solar exposure and warming, riparian buffers can serve a variety of functions to nearby streams such as reducing bank sediment erosion, providing plant and animal habitat, and providing a source of woody debris. On agricultural lands in King County, riparian areas have been extensively modified over many years and invasive reed canarygrass is dominant in many locations, although sections of some watercourses still maintain up to 90% native vegetation (U.S. Army Corps Of Engineers, 1997). This study does not address the function of those areas that still maintain up to 90% native vegetation, or the impact of maintenance and mitigation in those areas. Instead, this study focuses on the dominant reed canarygrass and Himalayan Blackberry vegetation. An understanding of minimum mitigation required to replace the shade benefits of these plants after maintenance will make maintenance and mitigation more economical, and preserve agricultural land.

9.1.1 Goals and Objectives

The goal of this project is to determine the impact of channel maintenance activities on the temperature of small agricultural watercourses by identifying the relative extent to which temperature is influenced by various maintenance design characteristics such as riparian vegetation, channel width, and channel side slope. With the assistance of KCDNRP staff, the following research hypothesis was posed in relation to this study component:

> Water temperature is not affected by changes in the cover density or type of bank vegetation.

Specific tasks required to accomplish the project goal and validate or repudiate the null hypothesis include:

- Identification of the impact of watercourse shade on water temperature.
- Identification of the effectiveness of Sitka willows, Himalayan Blackberry and reed canarygrass riparian vegetation in providing watercourse shade.
- Development and customization of a modeling tool to determine the water temperature impacts of various channel maintenance scenarios.
- Modeling diurnal temperature fluctuations to identify changes in water temperature produced by various channel maintenance confirmation. (Simulated data generated by the model will also be useful in modeling nutrient budgets and dissolved oxygen concentrations.)
- Collection of field data to support model development, calibration and verification.

The focus of this study was to identify minimum, cost efficient mitigation for watercourse maintenance. Consistent with the intended purpose, this study focused on identifying the shade benefits provided by existing vegetation versus vegetation typically planted for mitigation purposes. Vegetation types that commonly exist along small agricultural watercourses in King County prior to watercourse maintenance include reed canarygrass (*Phalaris arundinacea)* (RCG) and Himalayan Blackberry *(Rubus discolor).* Willows such as Sitka willow (*Salix Sitchensis*) are commonly planted as part of mitigation that follows maintenance. This study focused on thermal impacts because temperature is the fundamental water quality parameter and can significantly determine a water body's suitability for supporting aquatic life. Because water temperature influences all other water quality parameters, another critical function of water quality modeling is to support modeling efforts for other parameters such as dissolved oxygen.

9.2 Study Background

9.2.1 Literature Review

Contemporary stream temperature models rely on physically based energy balance and mass transport equations to mathematically describe the processes that drive stream system behavior (Shepard, 2005). Empirical models are equations that relate a selected number of measured input parameters, such as ambient air temperature, to an observed response, such as water temperature. The components of empirical models may not have a direct meaning in physical reality. Empirical models are not necessarily applicable to locations or systems other than the one for which they were developed while models based on the laws of physics are true everywhere. Empirical models are appropriate when the physical mechanisms that determine system response are not known. While no temperature model is entirely physically based, entirely empirical temperature models are not well suited for identifying the impact of changes in individual physical watercourse characteristics such as channel width, depth, or the distance from the watercourse to shading vegetation on its bank.

Bormann (2000) lists 45 environmental and physical factors influencing stream temperatures. Among these factors are weather conditions such as air temperature, relative humidity and wind speed, stream site physical characteristics such as stream width, depth and roughness, and the presence of shading vegetation and topography. Brown (1969) initially identified the importance of forest cover in protecting stream temperature caused by an increase in the stream's exposure to solar radiation. He compared water temperature at the outlet of streams running through forested and harvested watersheds over two years and found that clearcutting increased the daily change in temperature by 14 degrees Fahrenheit in the month of August. Brown (1969) applied the heat energy balance method to small streams and pointed out the utility of temperature modeling in managing stream temperature. Brown (1969) pointed out that because small streams carry smaller volumes of water, the temperature of small streams is more responsive to net energy exchange than larger rivers and therefore more accuracy is required of an energy balance models applied to small streams in order to achieve a given accuracy in temperature prediction.

Energy balance methods account for predicted incoming and outgoing heat fluxes in order to derive an estimate of the net flux of energy received by a segment of water in a stream. The following equation is a general energy balance equation similar to the one used by Brown (1969):

$$\Phi_{total} = \Phi_{solar} + \Phi_{longwave} + \Phi_{evaporation} + \Phi_{convection} + \Phi_{streambed} \quad (9.1)$$

where Φ_{solar} is the sum of shortwave direct and shortwave diffuse solar radiation penetrating the stream's surface, $\Phi_{longwave}$ is the sum of long-wave solar radiation reaching the water's surface through the canopy opening and streamside vegetation, $\Phi_{evaporation}$ is the flux representing heat loss due to evaporation, $\Phi_{convection}$ is the heat flux due convection at the air water interface, and $\Phi_{streambed}$ is the flux experienced due to conduction between the water column and stream bed. The range of magnitudes of the heat flux terms described, have been outlined by Martin and McCutcheon (1999). According to Martin and McCutcheon (1999), shortwave solar radiation

ranges from approximately 50 to 500 W/m^2, long wave atmospheric radiation ranges from approximately 30 to 450 W/m^2, long wave radiation emitted from a water body ranges from approximately 300 to 500 W/m^2, evaporative heat loss ranges approximately 100 to 600 W/m^2, convective heat exchange ranges approximately 100 to 600 W/m^2.

The change in stored energy determined by the balance of these fluxes is converted to a change in stream temperature. The amount of heat transferred by a flux is equal to the heat flux times the receiving area:

$$\Delta H = \Phi \cdot A \tag{9.2}$$

where ΔH is the heat energy transferred (calories/min), Φ is the heat energy flux (cal/m^2-min), and A is the receiving area (m^2). A general equation for the change in water temperature due to heat exchange with the environment is as follows (Martin and McCutcheon 1999)[1]:

$$\frac{\partial T}{\partial t} = \frac{\Phi_{total} \cdot A_s}{\rho_{water} \cdot c_{p(water)} \cdot V} \tag{9.3}$$

where T is the water temperature (°C), ρ_{water} is the density of water (kg/m^3), $c_{p(water)}$ is the heat capacity of water (cal/kg-°C), V is the volume of water (m^3), A_s is the stream surface area (m^2), and Φ_{total} is the total heat flux (cal/m^2-min).

Brown (1969) attained temperature predictions within ±1°F with his energy balance method using site specific measured meteorological and solar radiation data. He noted the importance of onsite meteorological data as well as a source of error introduced by the use of data that does not accurately reflect the attenuation of solar radiation due to shade from riparian vegetation. Since this time, numerous other researchers have studied and documented the benefits of riparian vegetation at reducing peak temperatures (Brown 1970, Klein 1979, Bartholow 1989, LeBlanc and Brown 2000, Johnston 2004). In a study of small, unshaded streams in Oregon, Brown (1970) determined that approximately 95% of the mid-day heat input was attributable to solar radiation. Summarizing the works done by numerous researchers including Levno and Rothacher (1967), Kopperdahl et al. (1971), Swift and Messer (1971), Barton et al. (1985), Beschta and Taylor (1988) and Amaranthus et al. (1989), Bartholow (2000b) concluded that loss of riparian vegetation lead to increases in mean water temperatures of 3-6^{o}C. Although much of the previous work has been related to forests with considerably longer stream segments, the general trends and conclusions appear to be applicable to agricultural waterways in King County. Since a small watershed in these studies was defined as 150 acres, the magnitude of temperature changes in the much shorter agricultural waterways should not be assumed to be as significant. Furthermore, as stated by LeBlanc and Brown (2000), "while these studies underscore the

[1] Although the bed conduction flux included in the Φ_{total} term is not directly associated with the water surface area of a rectangular channel, the surface area of the stream segment is equal to the area of the channel bottom.

significance of riparian forest in water-temperature moderation, the results cannot simply be extrapolated to other stream environments."

Brown's application of the energy balance to small streams was followed by the development of several more detailed models using equations to predict solar radiation at the earth's surface. Bowie et al. (1985) summarized approaches developed by the Tennessee Valley Authority (1972), Ryan and Harleman (1973), the US Army Corps of Engineers (1974), Thomann et al. (1975), Baca and Arnett (1976), and Edinger and Buchak (1978). These models are less reliant on site specific solar radiation data in order to accurately predict water temperature (Martin and McCutcheon 1999). In 1972, Wunderlich presented an equation to calculate the shortwave solar flux reaching the earth's outer atmosphere as a function of solar altitude:

$$\Phi_{SRE} = \frac{\Phi_{SRC}}{r^2} \sin\theta_{sun} \tag{9.4}$$

where Φ_{SRC} is the extra terrestrial solar constant (cal/m^2-min), Φ_{SRE} is the direct solar radiation received at the earth's outer atmosphere (cal/m^2-min), θ_{sun} is equal to the solar altitude (radians), and r is the ratio of the earth to sun distance to the average earth to sun distance (dimensionless) as given by:

$$r = 1 + 0.017 \cdot \cos\left(\frac{2\pi}{365}(186 - TJ)\right) \tag{9.5}$$

where TJ is the Julian day plus day fraction (i.e., 1 PM would be an additional 13/24 of a day).

To predict the solar flux at the earth's surface, the attenuation and scattering of radiation in the earth's atmosphere must be accounted for. Ibqal (1983) describes shortwave solar radiation reaching the earth's surface as:

$$\Phi_{SRA} = \Phi_{SRE} \cdot Trans_{atm}^{M} \cdot \cos\theta_{zenith} \tag{9.6}$$

where Φ_{SRA} is the direct beam solar radiation routed through the atmosphere (cal/m^2), $Trans_{atm}$ is the transmissivity of the atmosphere (dimensionless), M is the optical airmass thickness (meters), and θ_{zenith} is equal to the solar zenith angle (radians).

The transmissivity of the atmosphere is described by:

$$Trans_{atm} = 0.0685 \cdot Cos\left(\frac{2 \cdot \pi}{365} \cdot (JD + 10)\right) + 0.8 \tag{9.7}$$

The optical air mass thickness in Equation 9.6 can be calculated as a function of the observer's elevation and the altitude of the sun as reported by Beschta and Weatherred (1984) using:

$$M = \left[\frac{\left(\frac{288 - 0.0065 \cdot elevation}{288} \right)^{5.256}}{\sin\theta_{sun} + 0.15 \cdot \left(\frac{180 \cdot \theta_{sun}}{\pi} + 3.855 \right)^{-1.253}} \right] \quad (9.8)$$

where elevation refers to the site elevation above sea level (meters). Following this general description of the energy and mass balance approach, is a more specific description of several commonly used stream temperature models.

9.2.2 Stream Temperature Models

9.2.2.1 TEMP86

The model TEMP86, by Beschta and Weatherred (1984), is a physically based model that predicts solar radiation at the earth's surface and estimates the interception of solar radiation by riparian vegetation. Beschta and Weatherred (1984) describe the attenuation of solar radiation by vegetation buffers using a cator that accounts for vegetation transmissivity. Like atmospheric transmissivity, vegetation transmissivity determines how effectively vegetation attenuates and scatters radiation before it can reach the water's surface. The equation is written as:

$$\Phi_{SolarVeg} = \Phi_{SRA} \cdot Transmissivity_{Veg}^{\ PathLength} \quad (9.9)$$

where $PathLength$ equals the distance radiation travels through vegetation before reaching the water's surface. A vegetation coefficient is used to calculate vegetation transmissivity as follows (Beschta and Weatherred 1984):

$$Transmissivity_{Veg} = 1 - 0.9 \cdot Vegetation_{coefficient} \quad (9.10)$$

where $Vegetation_{coefficient}$ is the vegetation coefficient representative of the buffer volume responsible for attenuation and scattering of radiation. The vegetation coefficient described by Beschta and Weatherred (1984) is not readily measurable in the field for application in temperature models because of the multitude of site and atmospheric conditions that can influence energy transfer and the lack of homogeneity within even relatively short study reaches (http://www.deq.state.or.us/wq/HeatSource/HeatSource.htm).

9.2.2.2 HSPF and the Model SHADE

An alternative method to describe attenuation of solar radiation by vegetation was developed by Chen (1996) with the model SHADE. Chen and Chen (1993) made an extensive comparison of stream temperature models and evaluation of their predictive capabilities to determine that none had full capabilities to dynamically simulate temperature on a watershed scale. As a result, Chen et al. (1998a,b) developed and tested a watershed scale stream temperature model including a stand-alone program called SHADE to dynamically adjust solar radiation data for water

temperature simulation within the model Hydrologic Simulation Program-Fortran (HSPF) based on vegetative and topographic shading characteristics. The SHADE model assumes that vegetation near the edge of the stream will overhang the active channel by ten percent of its width. The error introduced by this assumption will be largest in the case of streams with uniform riparian vegetation along with extensive or minimal overhang existing close to a small watercourse.

Chen (1996) applied the Beer-Lambert law (Martin and McCutcheon 1999), which states that absorbance is directly proportional to the solution concentration, to describe the extinction of solar radiation as it passes through riparian vegetation based on vegetation density. Chen's (1996) approach differs from that of Bestcha and Weatherred (1984) that instead of a vegetation coefficient, Chen's model requires vegetation density as an input, which can be observed either in the field or through analysis of aerial photographs. Chen's model is described as follows:

$$Shade_{Density} = 1 - \exp(-\lambda \cdot PathLength) \tag{9.11}$$

where $Shade_{Density}$ is the density of shadow cast by vegetation and

$$\lambda = -\frac{Ln\,1 - VegDensity}{VegH_{actual}} \tag{9.12}$$

To determine the amount of solar radiation reaching the water's surface, the length of a shadow cast on the water's surface is multiplied by its density to result in an effective shade length.

$$Shadow_{Length} = Shadow \cdot Shade_{Density} \tag{9.13}$$

where $Shadow$ is the actual shadow length and $Shadow_{Length}$ is the effective shadow length. Solar radiation received by the water's surface is then calculated as:

$$\Phi_{Veg} = \Phi_{SRA} \cdot \left(1 - \frac{Shadow_{Length}}{WWidth}\right) \tag{9.14}$$

Chen et al. (1997) successfully applied HSPF and the model SHADE in watershed scale modeling efforts. Stream temperature modeling on the Grande Ronde watershed was performed to provide guidance for riparian restoration activities (Chen et al. 1997). The SHADE model used topographical shade angles, and riparian vegetation dimension and location information to adjust global solar radiation reaching the stream's surface. HYDR, the hydraulic module of HSPF, calculates the wetted width of the stream on an hourly basis (Bicknell et al. 1997, Deliman et al. 1999). Stream bed conduction, although acknowledged to be a potentially important factor for smaller watercourse, is not addressed in this model. Among Chen's (1996)

conclusions is the assertion that natural weather cycles do not moderate stream temperature for the survival of salmon. Riparian vegetation is noted as the only potentially manageable factor that could significantly reduce lethal and sub-lethal temperatures. Chen (1996) was noted that wider channels could not be sufficiently shaded to reach target standards of maximum summer temperatures that do not exceed 16°C and seven day average maximum temperature that does not exceed 14.5°C. Model predictions showed that 41 out of 51 stream segments could reach target standards with restored vegetative buffers. Model accuracy was 2.6 to 3.0°C (Chen et al. 1997; Chen et al. 1998b).

9.2.2.3 Heat Source

Much of the methodology for modeling solar radiation above and below a riparian buffer used in TEMP86, as well as the riparian extinction coefficient proposed by Chen (1996) in the model SHADE, were later applied in the development of the model Heat Source. The first model Heat Source was a simple reach scale model, using the methods described by Beschta and Weatherred (1984) to account for the shade of riparian vegetation. Heat Source 6.0 applies Chen's model SHADE. Version 6 accepts dynamic weather and tributary temperature data but constant flow rates. Heat Source has since evolved into a watershed scale model (v. 7.0) capable of accepting data that represent great spatial detail in channel morphology and riparian vegetation as well as dynamic weather and stream flow data. One of the most significant challenges in applying this model is providing input data with the necessary spatial extent and degree of accuracy that the model can effectively utilize (Boyd and Kasper 2003). Hydrologic Simulation Program-Fortran and Heat Source 7.0 are detailed models suited to temperature predictions on a watershed scale and are less suited to the small watercourses of interest in this study.

9.2.2.4 SSTEMP

The Stream Segment Temperature Model (SSTEMP) is the reach scale version of SNTEMP, a steady state average daily model that uses physical relationships and vegetation density to predict solar radiation reaching the water's surface (Bartholow 2000a). Like many stream temperature models, it is hydraulically strictly steady state and does not attempt to consider changes in temperature with respect to depth or location across a stream cross-section. Change in temperature is modeled only in the downstream direction. Because it is an average daily model, the shortest possible time period for averaging is 24 hours. All inputs are in the form of daily to yearly mean values, and are applied uniformly over a reach. SNTEMP does not accept changing hydrological or meteorological data provided on a regular time step, and thus performs poorly where dynamic or diurnal behavior is of interest. This makes SNTEMP less suitable for calculating the effects diurnal temperature changes and is an important limitation of the model (Bartholow 2000a, Bartholow 2002).

Daily maximum temperature (or afternoon average stream temperature) is often of interest in the study of thermal pollution or temperature as a habitat-limiting factor. Because of the strong influence of ambient air temperature and weather conditions on stream temperature, SNTEMP approximates a maximum ambient temperature using an empirical equation to simulate fluctuations around the average daily input value. Since this empirical equation was developed and calibrated in a single watershed, it is not necessarily suited to all locations and should be modified and calibrated for use in other locations with different local conditions. In addition, SNTEMP's approach to calculating daily maximum or afternoon average temperature is likely to be a source of error despite calibration. The Stream Segment Temperature Model also makes the

assumption that the fluctuations in temperature from the daily average to the daily maximum are equal in value to the change in temperature between daily average and daily low temperature. In general, SNTEMP gives thorough treatment of each possible heat source and sink of heat including the influence of shade from topography and riparian vegetation. The primary sources of error in SNTEMP are daily averaging and the model's inability to accept meteorological data (Bartholow 2000a).

9.2.2.5 QUAL2E

The USEPA model QUAL2E has been used extensively and contains a basic hydrologic model. QUAL2E performs a quasi-dynamic analysis by accepting dynamic meteorological inputs with steady-state flow values. The model has the capability to accept changing meteorological data taken at a regular time interval, and to behave quasi dynamically for diurnal temperature simulation. QUAL2E also produces steady-state results if dynamic meteorological data is not available. In older versions of this software, meteorological information was applied equally to all locations in the watershed, but newer versions allow these data to vary spatially. Although QUAL2E can accept dynamic forcing functions such as ambient temperature and other meteorological factors, the hydrologic forcing functions must be constant. All flows and boundary conditions are constant for the QUAL2E model, as they are in SNTEMP. QUAL2E, despite its advanced quasi-dynamic capabilities, is lacking in consideration of factors shown to be potentially significant in modeling stream temperature. QUAL2E does not model riparian vegetation shading and neglects bed conduction (Brown and Barnwell 1987).

A new version of this model called QUAL2K is now available from the USEPA (2008). This model does allow for explicit hourly input of shade. The Washington State Department of Ecology developed a tool for calculating riparian shade to assist in the processing of input data; however, at the initiation of this project, this tool was not available. Consequently, while QUAL2K has subsequently been widely used, at the time this project began, HeatSource (rationale discussed in Section 9.2.4.1) was used.

9.2.3 Environmental Factors Driving Stream Temperature

Despite a large number of stream temperature studies, controversy exists regarding the effect of shade and riparian vegetation on water temperature. Larson and Larson (1997) suggest that the rate of stream temperature change can be attributed to the gradient in temperature between air and water, on the basis that air temperature is an indicator of the thermal environment. These authors also point out that difference in air temperature from high to low elevations is significantly due to the cooling of air as it expands at higher elevations where it is exposed to lower atmospheric pressure. Larson and Larson (1997) point out that flow velocity determines how long water is exposed to a particular thermal environment. They attribute changes in stream temperature as water flows from high to low elevations to the corresponding change in air temperature to which the stream is exposed. Larson and Larson (1997) do not mention solar radiation and shade as an additional significant factor in stream heating. They observe that at a minimum, flow velocity as well as air and water temperature above and below a reach of interest, should be measured in order to draw any conclusions about the influence of the environment on water temperature.

In a very simple experiment by Moore et al. (1999), equal water volumes with similar initial temperatures were placed into tanks insulated on the sides and bottom. One tank was exposed to

August solar radiation and one was completely shaded by tarps. The results showed that the shaded tank was significantly cooler over the course of the study, though the both tanks were exposed to the same ambient temperatures. A similar study conducted using running water produced similar results, demonstrating the potential importance of solar radiation and shade in determining water temperature (Petersen et al. 1999). This simple experiment affirms the potential importance of stream shade in models such as those developed by Beschta and Weatherred (1984), Chen (1996), Boyd and Kasper (2003) and others. The works of Beschta and Weatherred (1984) and Chen (1996) do not deny the importance of air temperature as one influence on water temperature, but rather include additional consideration for the streams' solar radiation exposure or sheltering.

9.2.4 Review of the Selected Water Temperature Model: Heat Source

9.2.4.1 Rationale for Heat Source Selection

Heat Source 6.0 was selected for adaptation and application in this reach scale study to identify the importance of riparian vegetation because of its treatment of riparian vegetation and meteorological conditions as well as its adaptability and ease of use. Heat Source 6.0 is a widely available share-ware program written in Visual Basic for applications in Excel. Heat Source 6.0 takes into account shading from topographical features and riparian vegetation. It simulates water temperature on an hourly basis, and accepts inputs of hourly weather data. It is designed to predict diurnal fluctuations in water temperature and is readily adaptable for use at the reach scale. This model also accepts detailed information describing the dimensions and density of riparian vegetation, including the vegetation's measured overhang length. Because Heat Source 6.0 is written in Visual Basic for Excel, the model does not require management or formatting of external data files to supply required data such as hourly weather data. Weather and other input data may be formatted and stored directly in the designated worksheet locations in the Heat Source model. This system is convenient since the input data used in simulation is stored with results and can be easily altered for the next scenario. Heat Source 6.0 was selected for use as the base model in this study to determine the impact of changes to channel characteristics and riparian vegetation associated with excavation for watercourse maintenance and subsequent mitigation plantings. Heat Source 6.0 was designed to accept daily continuous data and report a single day of simulation results, although the simulation may be repeated over several days, only the last day is stored and reported.

The riparian extinction method applied by Chen *et al*. (1998a) in the model SHADE is used to simulate shade in Heat Source 6.0. As presented by Tissue (2000), the Beer-Lambert Law (commonly known as Beer's Law) can be derived by approximating molecules in solution as opaque disks whose cross-sectional area σ_A represents the effective area seen by a photon of frequency w. Figure 9-1 represents an infinitesimal slab, *dz*, of sample:

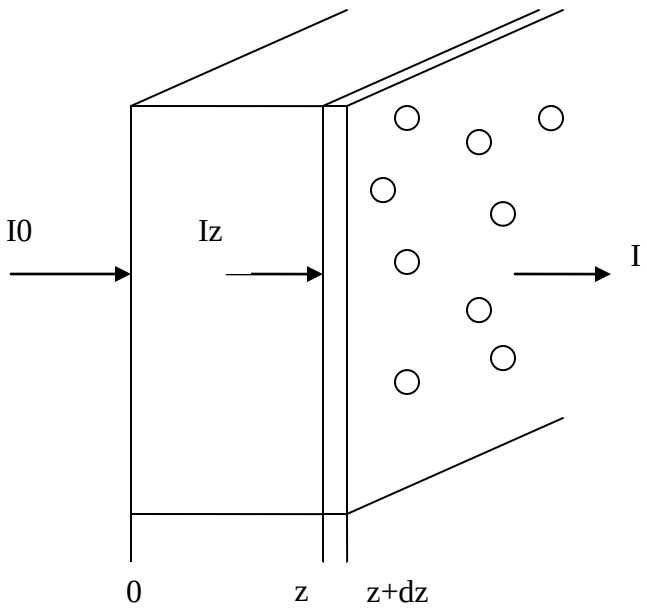

Figure 9-1. Conceptual differential volume used to illustrate the Beer-Lambert law

$$A_{0a} = \sigma_A \cdot N \cdot A \cdot dz \tag{9.15}$$

where A_{0a} is the total opaque area on the slab due to the absorbers, A is the sample cross-sectional area, I_o is the light intensity entering the sample at z = 0, I_z is the light intensity entering the infinitesimal slab at z, dI is the light intensity absorbed in the slab, I is the light intensity of light leaving the sample, σ_A is the cross-sectional area of a molecule represented as an opaque disk, and N is the number of molecules per volume.

The fraction of photons absorbed is represented as the fraction of absorbing area to total area as:

$$F_a = \frac{\sigma_A \cdot N \cdot A \cdot dz}{A} \tag{9.16}$$

where F_a is the fraction of photons absorbed.

The ratio of light intensity entering the slab to that leaving the slab is proportional to the fraction of photons absorbed.

$$\frac{dI}{I_z} = -\sigma_A \cdot N \cdot dz \tag{9.17}$$

Integrating from z = 0 to z = b gives:

$$\ln(I) - \ln(I_0) = -\sigma_A \cdot N \cdot b \tag{9.18}$$

or

$$-\ln\left(\frac{I}{I_0}\right) = -\sigma_A \cdot N \cdot b \tag{9.19}$$

Comparing this equation and with that from Chen et al. (1998a):

$$ShadeDensity = 1 - \exp(-\lambda \cdot PathLength) = 1 - Trans = 1 - \frac{I}{I_0} \tag{9.20}$$

where *Trans* is the transmissivity.

Applying this model to riparian vegetation, the element through which light passes, is the riparian buffer strip with length (*dx*) and height equal to the vegetation buffer. In Beer's Law above, N is the number of molecules per cubic centimeter and sigma represents the area of a molecule. When combined, these terms represent shaded area per cubic centimeter. In the infinitesimal volume, the total area shaded is the amount of area shaded per cubic centimeter, times the infinitesimal volume size, which is A *dz*. The fraction of photons absorbed is the ratio of this shaded area to the total area.

In the Beer's Law model (Oke 1978), the term $\sigma_A \cdot N$ is represented by the density of vegetation within the riparian buffer. This use of Beer's Law assumes that each vegetation object within the buffer is opaque. When vegetation density is observed for a modeled distance *dx*, aerial photographs are commonly used to identify the percentage of riparian buffer land area covered by vegetation for the distance dx. Because vegetation, such as a single tree or willow is not opaque, when complete canopy coverage is achieved over the watercourse, the vegetation density is the density of the vegetation type. Buffers selected for this study completely occupy the riparian zone, implying a density of 100%, with relatively constant buffer widths. It should be noted that shadows of varying densities are cast by different vegetation types due to differences in maturity and opaqueness. The Heat Source 6.0 model used in this study is capable of accounting for changes in opaqueness that occur over time as the vegetation matures if the user knows how to vary the appropriate coefficients. However, while representative vegetation was used in the calibration phase of this study, no attempt was made to determine the age of the vegetation.

In practice, aerial photographs are often used to estimate vegetation density based on the spatial density of vegetation objects observed in the riparian zone. This density is adjusted to account for variations in vegetative opacity using a classification system defined by vegetation type. For example, conifers may occupy the riparian zone at approximately an 80% density and thus conifers as a class might be assumed to have 90% density. Solar Pathfinder measurements are used in the field to validate model predicted Effective Shade values based on vegetation input data collected as described above. Effective shade is determined by the model as follows:

$$E_{shade} = \frac{\Phi_{atmospheric} - \Phi_{vegetation}}{\Phi_{atmospheric}} \quad (9.21)$$

If used in accordance with the user's manual, the Solar Pathfinder does not account for plant density during field measurement of summer month effective shade. In other words, vegetative shade of vegetation is treated the same as shade cast by buildings or solid structures. Any adjustment to account for diffuse shadows is at the discretion of the user. Solar Pathfinder measurements are typically made at the center of the watercourse at water level to account for bank topography. Vegetation typically has a great deal of spatial variation. Therefore, the point locations of field measurements of effective shade using a Solar Pathfinder are unlikely to coincide precisely with segment-averaged vegetation input data developed using the plant density and vegetation classification system described above. In addition, spatial variation in vegetative conditions is an even greater source of discrepancy between Solar Pathfinder measured effective shade and modeled effective shade values. Nonetheless, when the Solar Pathfinder is used to take a large number of measurements over a large spatial scale, such measurements have been shown to correlate well with predicted effective shade values. When spatial variation in vegetation is minimized or eliminated (as it is in a uniform continuous swath of vegetation along a single watercourse reach), the majority of error in estimating effective shade is the result of neglecting to account for diffuse shadows over portions of a study reach.

In accordance with Equation 9.1, Heat Source 6.0 describes the rate of temperature change in an element of stream water as the sum of the rate change in temperature due to advection, dispersion and heat energy flux. Heat Source 6.0 thus estimates the amount of energy exchanged between an element of water and its surroundings as a function of air temperature, channel bed characteristics, and solar radiation, which in turn is dependent on the time of day, time of year, the location of the element of interest on the earth and its orientation to the sun (Boyd 1996).

Evaporative heat flux represents loss of heat from the water column. Heat loss associated with evaporation is directly related to the latent heat of vaporization (LHV) of water. The rate of evaporation from the water column is determined according to an empirical relationship developed based on studies of evaporation from open channels. The rate of evaporation is a function of the vapor pressure deficit and wind speed and can vary according to many factors including wind sheltering by riparian vegetation.

Convective heat exchange is molecular heat exchange between water and air. Convective heat exchange is a function of the same parameters that influence evaporative heat loss, and can be expressed as a combination of an empirical ratio and the rate of evaporation. Stream bed conduction represents heat exchange between the water column and bed material. Bed conduction is a function of the equilibrium soil temperature, the depth over which the soil reaches equilibrium temperature and soil particle size. Solar radiation represented by the term Φ_{solar} , is determined through four sequential steps to determine the value of solar radiation flux at four locations along its path from the sun to the water column. Direct shortwave solar radiation is considered to radiate from the sun as a point source. The first step is to calculate the solar radiation at the earth's outer atmosphere. This value is referred to as extra-terrestrial solar radiation. This approximation is based on measured values of solar radiation and a trigonometric

relationship between the sun and a plane tangential to the earth (Wunderlich 1972). The second step is the calculation of solar radiation reaching the outer limits of riparian vegetation. In other words, how much radiation hits the surface (leaves) of the vegetation. This value is a function of atmospheric transmittance. The third step is to calculate the quantity of solar radiation that reaches the stream's surface, taking into account shading by the riparian vegetation. Finally, the fraction of the solar radiation that reaches the water's surface which is reflected from the water's surface as a function of the angle of incidence is calculated.

A second component of total solar radiation is shortwave diffuse solar radiation. When direct shortwave solar radiation reaches the earth's outer atmosphere, a fraction is reflected and redirected so that it is no longer considered as a point source, but instead is scattered to radiate in all directions. Shortwave diffuse solar radiation reaching the outer limits of riparian vegetation is estimated as an empirical function of extra terrestrial solar radiation. The methodology presented is similar to that reported by Beschta and Weatherred (1984). A fraction of the available diffuse solar radiation will reach the water's surface through openings in riparian vegetation. The remainder is considered to be blocked by vegetation. The total solar radiation reaching the water column is the sum of diffuse and direct shortwave solar radiation that passes the water's surface.

Long-wave, or thermal radiation, has a positive and negative component. Long-wave radiation is emitted by both the earth's atmosphere and the water column. Long-wave radiation emitted by the water column represents the negative component, while long-wave radiation emitted by the atmosphere and received by the water column constitutes the positive component. Like diffuse solar radiation, long-wave radiation is considered to radiate from all directions.

Recall that each of the last three energy balance components discussed -- direct shortwave solar radiation, shortwave diffuse solar radiation, and long wave radiation, have a unique interaction with riparian vegetation. These energy balance terms are will now be described in more detail as they are calculated in Heat Source 6.0.

9.2.4.2 Shortwave Solar Radiation

As solar altitude changes over the course of the day, solar radiation may be intercepted by distant topographic features before reaching the outer limits of the riparian buffer. Interception by distant topographic features is accounted for in Heat Source 6.0 by calculating the effects of such features in relation to the local time. After the sun has risen over topographic features solar radiation may be intercepted by stream bank vegetation, or the stream bank itself if the stream's surface elevation is lower than the top of the bank. The vertical distance from the stream's surface to the top of the bank must be measured in the field. For any shading feature, an angle can be calculated between the level of the water's surface and the top of the shading feature. This angle is a function of the height of the object and its distance from the mid-point of the water's surface. The model determines that a shadow is being cast by the bank or vegetation by comparison of vegetation and topographic angles with solar altitude. The length of a shadow is calculated based on the geometry of riparian vegetation and the sun's position. This length is referred to as the shadow width, and is assumed to be cast only by vegetation on the sunward bank.

The riparian area is described by the type and the dimensions of vegetation comprised of consecutive strips of vegetation with user defined widths that parallel water's edge. Zone 0 is the

watercourse bank itself, and can also be defined as the zone between the water's edge and water ward edge of the riparian vegetation. For the purposes of this study, the bankfull width is defined as width between the tops of the bank. Bankfull width must be identified in the field as the point where there is a break in slope between the sides of the watercourse banks and relatively level floodplain. The transverse distance from the water's edge to the bankfull mark is calculated as follows:

$$Transverse_0 = \frac{Bankfull_{Width} - Wetted_{Width}}{2} \tag{9.22}$$

where $Transverse_0$ is the distance from the water's edge to the bankfull mark (meters) as defined by the high water stage resulting from the 2-year return flow event. The length of shadow cast by the sunward bank itself is first approximated:

$$Shadow_{widthBank} = \frac{Incision \cdot \sin\left|\theta_{azimuth} - \theta_{aspect}\right|}{\tan\theta_{sun}} \tag{9.23}$$

The length of shadow cast by the stream bank that exists only on the water's surface is equal to this shadow length minus the transverse distance. If the shadow length minus the transverse distance is still greater than the wetted width, the fraction of the water's surface covered by the bank's shadow is set to 1. Zone 1 is the first riparian vegetation zone. Vegetation, if it exists in this zone, is assumed to exist at the top of the bank at the bankfull elevation. Riparian vegetation may exist between banks, but this component of vegetation is considered overhanging. Riparian vegetation has some branches that extend waterward beyond the top of bank. In order to predict shadow length and the amount of the water's surface shaded by vegetation, the transverse distance from the water's edge to the leading edge of riparian vegetation is calculated as follows:

$$Transverse_1 = Transverse_0 - Veg_{Overhang} \tag{9.24}$$

If $Veg_{Overhang}$ is greater than $Transverse_0$, a negative number would result. The transverse distance from the water's edge to the leading edge of vegetation, $Transverse_1$ is instead set to zero. This describes vegetation that begins at the water's edge.

Using a program loop, the shadow length cast by vegetation in each zone on the sunward bank, is calculated using:

$$Shadow_{width} = \frac{VegH_{apparent} \cdot \sin\left|\theta_{azimuth} - \theta_{aspect}\right|}{\tan\theta_{sun}} - transverse(zone) \tag{9.25}$$

where $transverse(zone)$ is the transverse distance for the particular zone.

The effective shade density of a shadow cast by riparian vegetation is calculated according to the methodology described by Chen et al. (1998a). Using Beer's Law (Oke 1978), the procedure can

be summarize in three steps. First, a riparian extinction coefficient (λ) for the vegetated zone is computed. Second, the average path length of the sunlight through the buffer is determined. And then, the third step combines this information into an equation for effective shade density. Details are provided below.

The length of this shadow over the water's surface is determined for each zone as the shadow length minus the transverse distance from the water's edge to the leading edge of that zone. The density of each shadow cast by vegetation is a function of the density of vegetation and the path length through vegetation as described by Chen et al. (1998a):

$$\lambda = -\frac{Ln\left(1 - VegDensity\right)}{VegH_{actual}} \tag{9.26}$$

where λ is the riparian extinction coefficient (m^{-1}), VegDensity is the vegetation density typically estimated from aerial photographs as the percentage of land in the riparian zone occupied by vegetation (dimensionless), and $VegH_{actual}$ is the height of riparian vegetation (meters).

A uniform vegetated zone width, and therefore a path length at any point in time, is assumed for a single differential distance using:

$$PL_{veg} = \frac{Veg_{width} + Veg_{overhang}}{\left|\sin\left|\theta_{azimuth} - \theta_{aspect}\right|\right| \cdot \cos\theta_{sun}} \tag{9.27}$$

where Veg_{width} is the width of vegetation from the bankfull edge perpendicular to the bank (meters) and PL_{veg} is the approximated path length of solar radiation through riparian vegetation (meters).

The fraction of the water's surface shaded by the bank receives no solar radiation. Solar radiation received by the fraction of the water's surface shaded by vegetation is determined for shadows cast by each zone as follows:

The Solar radiation flux in the shade of vegetation is calculates as:

$$\Phi_{shadedVegetation} = \Phi_{SRA} \cdot \alpha_{shadedSunward} \cdot \left(1 - Shadow_{densitySunward}\right) \tag{9.28}$$

Solar radiation on the unshaded fraction of the stream's surface is calculated as:

$$\Phi_{unshadedFraction} = \Phi_{SRA} \cdot (1 - \alpha_{shaded}) \tag{9.29}$$

where the total fraction shaded is the sum of the fractions shaded by the bank and sunward vegetation.

Direct beam shortwave solar radiation routed to the stream surface is calculated as the sum of the solar radiation flux received by the shaded and unshaded fractions of the water's surface:

$$\Phi_{SRV} = \Phi_{shadedVegetation} + \Phi_{unshadedFraction} \tag{9.30}$$

Recall that a fraction of diffuse solar radiation will arrive at the stream's surface through the openings in the canopy. The remaining fraction of diffuse radiation is assumed to be blocked by the stream bank and bank vegetation. The fraction of diffuse radiation that reaches the water's surface is proportional to the fraction of a 180 degree view along a line that extends from the left bank horizon (0^o) directly overhead (90^o) to the right bank horizon (180^o) that is unobstructed by vegetation. This fraction is the View_To_Sky. The minimum open sky view for each bank VTS_{Bank} is used in determining the amount of radiation that passes through the riparian vegetation or the opening in the canopy. The open sky view is the sum of the minimum open sky view for the right and left halves of the channel cross-section.

$$VTS_{Bank} = \frac{180}{\pi} \cdot \tan^{-1}\left(\frac{VHeight_{apparent}}{transverse(z)}\right) \tag{9.31}$$

where $transverse(z)$ equals the distance from the center of the stream to the leading edge of the zone.

The fraction of a 180° field of view that is open to the sky is calculated as follows:

$$View\_To\_Sky = \frac{VTS_{Bank1} + VTS_{Bank2}}{180} \tag{9.32}$$

The amount of diffuse solar radiation reaching the water's surface through the canopy opening is calculated as follows:

$$\Phi_{SDVO2} = \Phi_{SDA} \cdot View\_To\_Sky \tag{9.33}$$

The total of direct and diffuse solar radiation passing the water's surface is:

$$\Phi_{TDS} = \Phi_{SRW} + \Phi_{SDVO2} \tag{9.34}$$

9.2.4.3 Longwave (Thermal)

Recall that the longwave radiation reaching the water's surface is the sum of radiation through the canopy opening and through the streamside vegetation calculated separately. Longwave radiation through the canopy opening is determined separately for the right and left halves of a channel cross-section. The equations used for the right and left banks respectively are:

$$CSR = 0.5 \cdot View\_To\_Sky \cdot (1 - (1 - 0.9 \cdot VegDensityR))^{Veg_{width}} \tag{9.35}$$

$$CSL = 0.5 \cdot View\_To\_Sky \cdot (1 - (1 - 0.9 \cdot VegDensityL))^{Veg_{width}} \quad (9.36)$$

where $VegDensityR$ equals the density of vegetation on the right bank and $VegDensityR$ is the density of vegetation on left bank.

$$\Phi_{longwaveVegO} = \left[1 - \left(\frac{CSR + CSL}{180}\right)\right] \cdot \Phi_{LongwaveATM} \quad (9.37)$$

The description of the View_To_Sky parameter is described in Equations 9.31 and 9.32. We would like the term:

$$\left[1 - \left(\frac{CSR + CSL}{180}\right)\right]$$

to range from a number close to zero, when the View_To_Sky is zero, to a value close to 1 when the View_To_Sky is 1. The maximum value for both CSR and CSL is 0.5. The maximum value for the term:

$$\left(\frac{CSR + CSL}{180}\right) \text{ is } \left(\frac{1}{180}\right)$$

so the minimum value for the term:

$$\left[1 - \left(\frac{CSR + CSL}{180}\right)\right] \text{ is } \left[1 - \left(\frac{1}{180}\right)\right] = 0.995 .$$

The value of the term:

$$\left[1 - \left(\frac{CSR + CSL}{180}\right)\right]$$

ranges from 0.995 to 1. This equation was adapted as described in Equation 9.28.

Long-wave radiation emitted by riparian vegetation is calculated as:

$$\Phi_{longwaveVeg} = \left[0.95 \cdot \left(\frac{CS0 + CS1}{180}\right) \cdot 0.95 \cdot \sigma \cdot T_{air} + 273.2^4\right] \quad (9.38)$$

The total atmospheric long wave radiation flux at the water's surface is calculated as the sum of long wave radiation that passes through vegetation and openings in the canopy:

$$\Phi_{longwave(+)} = \Phi_{longwaveVeg} + \Phi_{longwaveVegO} \quad (9.39)$$

9.2.4.4 Stream Bed Conduction

Heat Source 6.0 methodology includes an energy balance on the stream bed, where the fraction of the stream bed composed of bedrock may absorb solar radiation routed through the water column. A fraction of this absorbed energy may be transferred back to the water column by:

$$\Phi_{TSB} = \Phi_{TDS} \cdot Trans_{stream}^{PLwater} \quad (9.40)$$

Solar radiation reaching the stream bed may be absorbed by bedrock and a fraction of the energy absorbed may again be re-absorbed by the water column. The solar flux absorbed by the watercourse bed is described as follows:

$$\Phi_{absorbed} = \frac{\Phi_{TSB} \cdot 0.53 \cdot BEDROCK}{100} \quad (9.41)$$

The above model for the absorption and radiation of heat energy by stream bedrock was developed by Sellers (1965) and cited by Beschta and Weatherred (1984) and others. The conduction flux, returning stored bed energy to the water column is then calculated as follows:

$$\Phi_{conduction} = \frac{E_{bed}}{14400} \quad (9.42)$$

where $\Phi_{conduction}$ is the conduction flux for one minute of the day (cal/m^2).

The stream bed energy balance is represented by the balance of incoming solar radiation energy absorbed, and conduction flux returned to the water column.

$$E_{bed} = \int (\Phi_{absorbed} - \Phi_{conduction}) \cdot dt \quad (9.43)$$

where E_{bed} is the energy stored in the bed (cal/m^2).

9.2.4.5 Flow Model

Heat Source 6.0 uses Manning's Equation to estimate flow velocity and depth at every distance step given discharge and assumed channel wetted width. The model assumes a rectangular channel, although most agricultural channels are in fact trapezoidal. The wetted width is assumed to be equal to 80% of the measured Near Stream Disturbance Zone (NSDZ) width. The NSDZ width is the width that can be measured between vegetal clearings on the left bank indicated by evidence of high flows such as drift lines. Measured flow values for each distance step are defined user inputs.

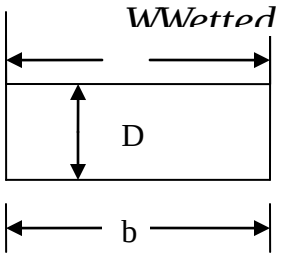

Figure 9-2. Water column and channel cross-section dimensions for Manning's flow model

Assuming that the hydraulic radius can be approximated by the depth of flow and the wetted perimeter can be estimated by the top width, Manning's equation for flow can be rearranged as:

$$D = \left[\frac{Q \cdot n}{\delta \, S^{1/2} \cdot WWetted} \right]^{3/5} \tag{9.44}$$

where Q is the discharge (m^3/s), δ is a units conversion factor equal to 1.0 for metric units, S is the channel gradient (dimensionless), n is Manning's roughness coefficient, and $WWetted$ is the water top width (meters) assumed to be given by:

$$WWetted = 0.8 \cdot NSDZ \tag{9.45}$$

Similarly, the flow velocity (meters/second) in the longitudinal x-direction (V_x) is given by:

$$V_x = \frac{\delta}{n} \cdot R^{2/3} \cdot S^{1/2} \tag{9.46}$$

where R is the hydraulic radius (meters) as given by:

$$R = \frac{area}{wetted\ perimeter} \approx D \tag{9.47}$$

Assuming a rectangular channel, the general equation describing the change in temperature due to the energy flux from the environment and advection from the upstream element is:

$$\frac{\partial T}{\partial t} = -V_x \cdot \frac{\partial T}{\partial x} + \frac{\Phi_{total}}{\rho_{water} \cdot c_p \cdot D} \tag{9.48}$$

where T is the water temperature °C, t is time, ρ_{water} is the density of water (kg/m^3), $c_{p(water)}$ is the heat capacity of water (cal/kg-°C), V is the volume of water (m^3), A is the area associated with the heat flux (m^2), Φ_{total} is the total heat flux (cal/m^2-min), and D is the watercourse depth (m).

9.3 Study Area

Figure 9-3 shows the geographic locations of the five Agricultural Production Districts (APDs) within King County Washington. The watercourses that drain excess flood water from King County's agricultural land are a combination of constructed drainage watercourses and natural or channelized streams. Agricultural drainage watercourses are typically low gradient within the flood plains of various valleys.

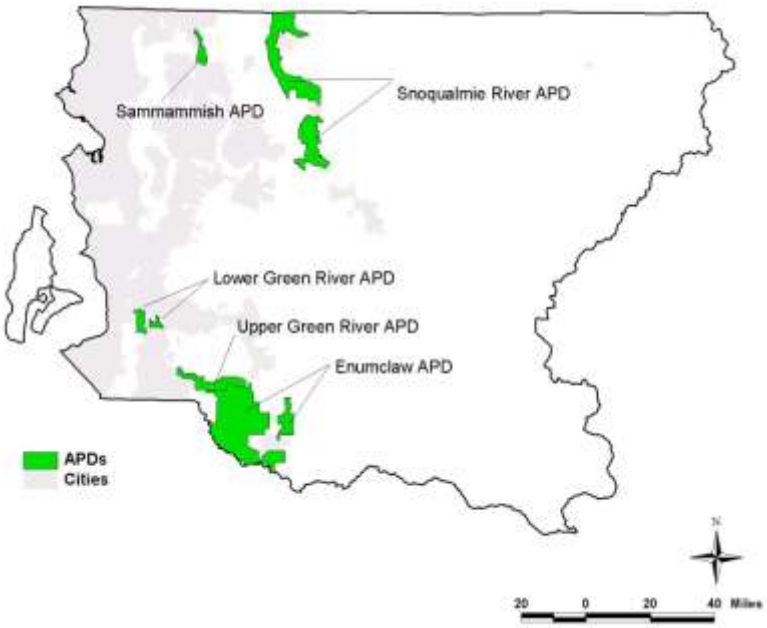

Figure 9-3. Map of King County Agricultural Production Districts (APDs)

Typical flow conditions in King County's agricultural drainage watercourses are characterized by winter flooding of agricultural land followed by low summer flows obstructed by emergent reed canarygrass (*Phalaris arundinacea*) and accumulated sediment. The riparian areas adjacent to these channels have been extensively modified over the years, and invasive reed canarygrass

is dominant in many locations, although sections of some watercourses are still surrounded by dense stands of up to 90% native vegetation (U.S. Army Corps Of Engineers, 1997). Native riparian plant communities in the Puget lowlands commonly comprise big-leaf maple (*Acer macrophyllum*), red alder (*Alnus rubra*), Oregon ash (*Fraxinus latifolia*), Sitka spruce (*Picea sitchensis*), black cottonwood (*Populus balsamifera* spp. *trichocarpa*), western red-cedar (Thuja plicata), red-osier dogwood (*Cornus stolonifera*), salmonberry (*Rubus spectabilis*, var. *spectabilis*) native rose species (*Rosa* spp.), and several willow species including Pacific, Sitka, and Hooker willows (Salix *lucida var. lasiandra, S. sitchensis and S. hookeriana, respectively.* Riparian areas that have been vegetated by past maintenance and channelization may also be vegetated by a mixture of native and non-native wetland emergent species including common cattail (*Typha latifolia*), sedges (*Carex* spp.) and rushes (*Juncus* spp.), as well as native and non-native grasses including Fecsues (*Festuca spp., mannagrasses (Glyceria* spp., foxtails (*Alopecurus* spp., velvetgrasses (*Holcus* spp.) and reed canarygrass (RCG) (*Phalaris arundinacea*). Because of their history of disturbance, the type of vegetation dominating the vast majority of the study sites is the non-native and highly invasive species, RCG. In addition, some channels are bordered by dense stands of two non-native blackberry species, Himalayan blackberry (*Rubus discolor*) and evergreen blackberry (*Rubus laciniatus*).

The height, density and width of the riparian vegetated corridor along agricultural channels, along with the vegetation's proximity to the water's edge and the amount of channel overhang, are the factors that determine the effectiveness of riparian vegetation in providing shade. Sitka willow is a multistemmed shrub that grows to heights of up to eight meters; specimens more than eight years old and five meters tall were found in the riparian zones of some of the study sites. Sitka willows planted immediately following channel maintenance projects were measured at heights nearing two meters tall and forming clumps of cover up to 1.5 meters in diameter two years after two growing seasons. Himalayan blackberries growing along watercourses were measured at heights of approximately 1.5 meters and 4 meters in diameter. Reed canarygrass was found growing on watercourse banks to heights of approximately 1.2 meters (although it was not uncommon to find 2 meter tall stands of RCG at the end of the growing season) and forms extensive monocultures that often occupied most of the adjacent farm fields.

Lowland King County's maritime climate is moderate and moist. Average annual rainfall is approximately 35" per year, with light, relatively continual rainfall throughout the rainy season from October through April. The average summer temperature is 64 °F with temperatures exceeding 90 °F only a few days per year. Winter temperatures rarely drop below freezing according to temperature records compiled for SeaTac International Airport compiled by the National Climatic Data Center (NCDC, 2003).

9.4 Methods

9.4.1 Site Selection and Field Data Collection

Field data were collected at sites representing various vegetation types in order to validate the temperature model. For the purposes of model validation and simulation, the focus of this study is limited to summer months, when flood flows have typically receded. Water quality is most critical during the summer, when air temperatures are the highest, and flows are lowest. This

period represents the greatest potential risk to habitat quality for salmonid fish. During these low-flows conditions, water generally moves at slow velocities, less than 1 foot per second, and is contained within watercourse banks where it is influenced by riparian vegetation in full foliage rather than occupying the agricultural flood plain. As a result, the same period that represents the greatest risk to salmonid habitat also represents the time when vegetation planted during mitigation may benefit water quality the most.

Study reaches were selected on the basis of relatively uniform water course widths, depths, and vegetation types for a minimum length of 100 meters. Reaches were selected with willows, blackberry, or reed canarygrass growing uniformly along the banks. Because the availability of uniform reaches was limited, channel dimensions such as side slope, width and depth were not selected. The morphology of selected reaches was controlled by the vegetation and uniformity criteria. The maximum reach length studied was 380 meters. Field monitoring consisted of on-site collection of weather data, including direct solar radiation, relative humidity, wind speed and air temperature. Air temperature data were collected at a weather station located on site as well as by Onset Optic Stowaway^{TM} temperature sensors located in the shade of riparian vegetation. Stream temperature data were collected by installing temperature sensors upsteam and downstream of the study reaches in the shade of riparian vegetation. Stream discharge was estimated using a Sontek Flow Tracker to measure velocity. Channel morphology information was collected through field measurements as well as survey data provided by King County. Local topographic shade angles were estimated using topographical maps. The dimensions of riparian vegetation were measured using a measuring tape.

Effective shade cast by vegetation was measured using a Solar Pathfinder below the vegetation but above the bankfull height at the mid point of the water's surface. Effective shade was greater than 90% for the reaches studied. Solar radiation was also measured under the vegetation canopy at bankfull level using a CM2 Campbell Scientific pyranometer. Pyranometer measurements were made above the mid point of the water's surface. Reaches were broken into 20 meter segments for pyranometer measurements. At the mid point of each segment a grid approximately 20 inches square, was used to select the position of pyranometer measurements. The grid contained 25 numbered cells. Pyranometer measurements were made below vegetation at cell positions according to a pre-made list of random cell numbers ranging 1 to 25. Measurements were made at a single grid location for approximately fifteen minutes. A corresponding measurement was then made using the same method, outside of the narrow riparian buffer to determine potential solar exposure. The average of solar radiation measurements made inside and outside of the vegetated buffer for each 20 meter segment was used to approximate effective shade. The approximate locations of experimental reaches are highlighted in yellow in the following site maps.

A map of the approximate location of a validation reach located South of the city of Duvall, Washington is presented in Figure 9-4. The site had reed canarygrass vegetation growing both emergent and on the banks. This reach is approximately 360 meters in length and demonstrated characteristic slow flows found in obstructed low gradient watercourses. A small tributary to the site was unmonitored during validation, representing unknown error. The tributary was visibly contributing no flow during the short period of temperature validation.

A map of the approximate location of a reach used for model validation located north of Enumclaw, Washington is presented in Figure 9-5. This site had mature willows growing along one bank. The overhang from these willows reached completely across the water's surface to the opposite bank, providing shade throughout the day. Local landowners indicated that the willows were approximately eight years old. The distance between willows at their base varied between approximately six feet and approximately two feet, however, apparent branch and leaf density was relatively uniform throughout the reach indicating that foliage occupied the reach more uniformly than the spacing of plantings. This reach was approximately 100 meters in length.

Figure 9-6 shows a map of a site used for validation located south of Kent, Washington. This site was approximately two hundred meters long and featured reed canarygrass growing both emergent and on the watercourse banks. This site demonstrated the characteristic slow flows and low gradient of an obstructed watercourse. Dense mats of reed canarygrass growing at the water's surface acted as a complete barrier to solar radiation in some locations along the reach. Typically reed canarygrass grew emergent from the watercourse at high densities.

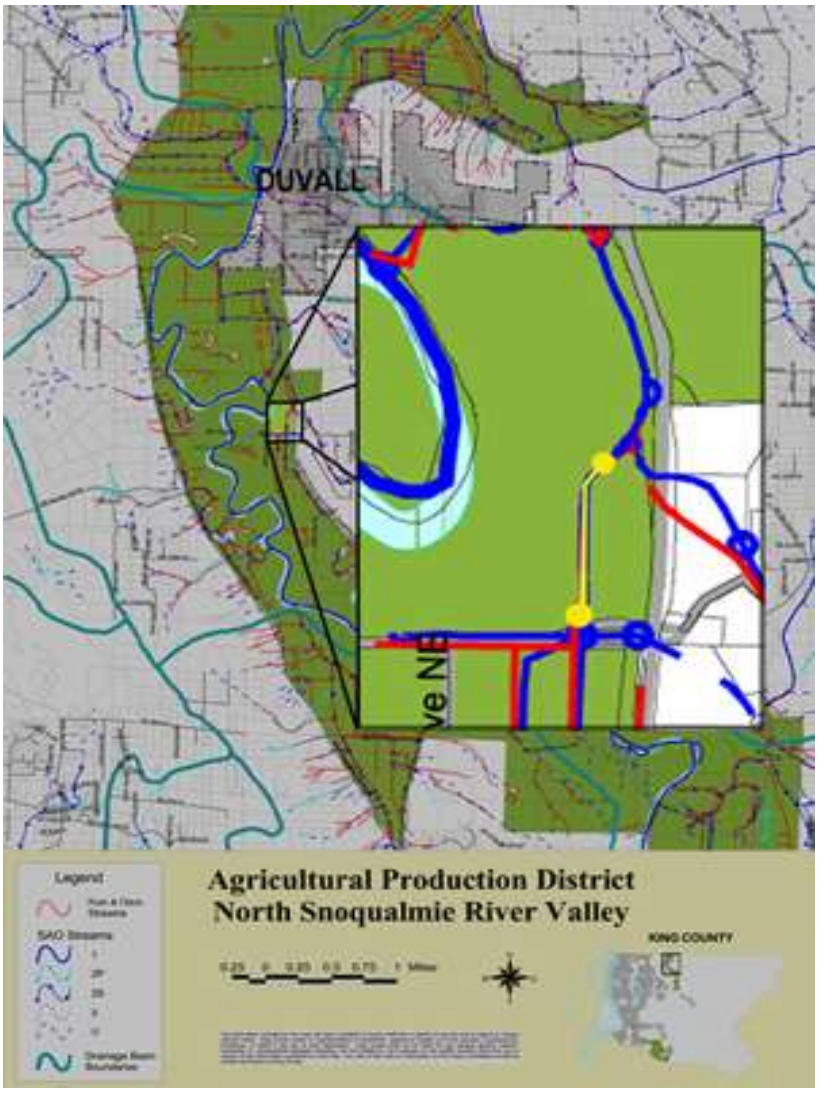

Figure 9-4. Heat Source model validation Site 1 map

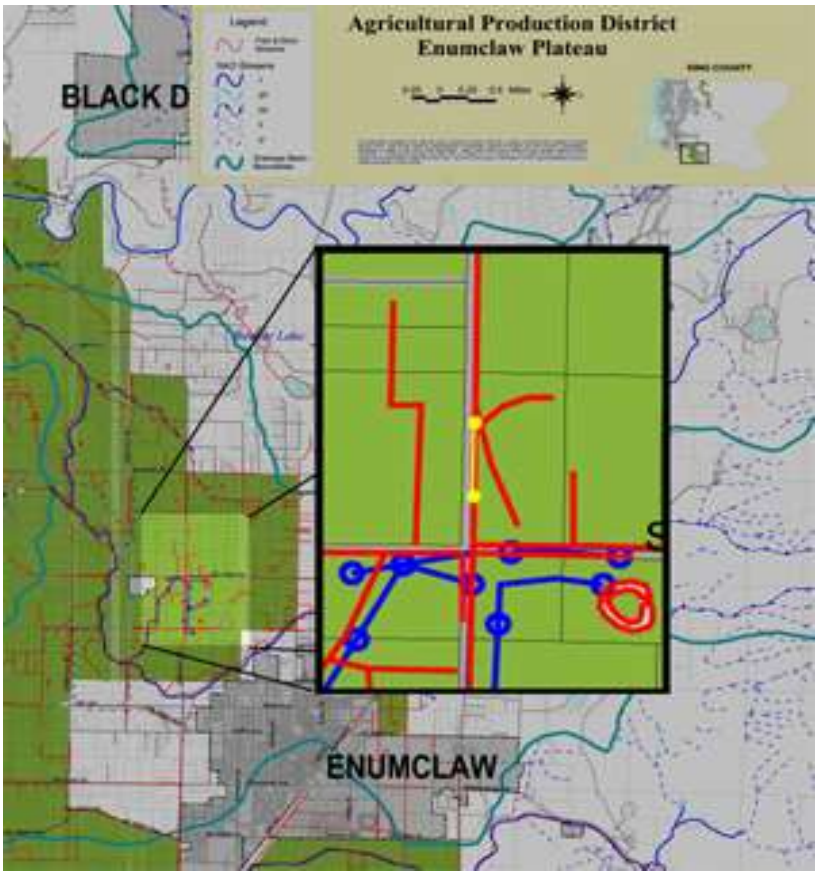

Figure 9-5. Modified Heat Source model validation Site 2 map

Figure 9-6. Modified Heat Source model validation and development Site 3

9.4.2 Field Data Limitations

Watercourse dimensions cannot be precisely defined in obstructed watercourses with dense reed canarygrass and a deep accumulation of fine organic sediment. The watercourse bottom is not visible and difficult to distinguish by feel due to the slow gradation between semi-suspended colloidal matter and settled material. For the purposes of flow velocity measurement and discharge estimates, the wetted width was approximated by the region where visible or measurable flow velocity could be detected. Measured or estimated flow velocities for the months of July and August were less than 1 foot per second in low gradient agricultural drainage watercourses. For modeling purposes, the wetted width potentially receiving radiation through emergent vegetation is the distance between solid vegetated boundaries on either bank. The depth of the bed conducting layer is represented by the depth of accumulated sediment over the firm channel bottom. In July of 2003, stream bed temperature data was collected by planting an Optic Stowaway temperature sensor approximately four inches deep, into the firm channel bottom. 13.7°C average temperature with diurnal sediment temperature fluctuation of approximately 0.3°C was observed.

9.4.3 Adaptations to the Model Heat Source

9.4.3.1 General Model Modifications

As mentioned above, Heat Source 6.0 was selected for use as the base model in this study to determine differences in the effectiveness of various riparian vegetation types in providing watercourse shade as well as the impact of shading vegetation on watercourse temperature. Research was conducted on a reach scale with water temperatures being monitored upstream and downstream from the study reaches. The study reaches were selected to meet the criteria of vegetative uniformity; each reach represented a single type of relatively uniform vegetation and exhibited the greatest possible uniformity in channel width and depth. The Heat Source 6.0 methodology was customized to predict temperature in small, low-gradient watercourses with a minimum of input data for application to reach-scale agricultural channel maintenance projects, which typically includes vegetative plantings intended to mitigate project impacts on existing riparian plant communities by shading to the stream in the future. Onsite air temperature and instream water temperature measurements taken upstream and downstream from each reach were used to validate and further develop the Heat Source 6.0 model. In addition, the Manning's equation flow model in Heat Source 6.0 was altered to represent a trapezoidal channel with user defined dimensions since project design for maintenance and mitigation projects typically requires a specified channel side slope. The modified Heat Source 6.0 model is intended for use in identifying the effects of various changes in watercourse characteristics, including mitigation plantings, associated with maintenance of agricultural drainage watercourses. The assumption that reach-scale characteristics are relatively uniform and representative of the selected study reaches allows the model to show a response to one condition applied uniformly. A wetland Manning's flow model was incorporated into the model to represent RCG and sediment obstructed low gradient channels, and adjustments were made to the shade model to best represent the shade cast by small stands of vegetation along small low-velocity watercourses.

The primary user interface for the modified model is the Inputs worksheet. The first column on the worksheet presents a set of labeled input cells where fixed input data including reach length, simulation start date, reach latitude, reach longitude, reach aspect, reach elevation, riparian zone width, channel side slopes, channel bottom width, water depth, depth of channel incision,

topographic shading angles to the west, south, and east, Manning parameter, channel slope, and simulation duration are entered. The user must then select a type of vegetation from the drop down box for the right and left channel banks as observed when looking upstream. To select the wetland flow model, the user can check a box labeled "channel obstructed by reed canarygrass". If emergent reed canarygrass is providing watercourse shade, the user should check the box labeled "Emergent Veg". The default type of emergent vegetation is reed canarygrass. To change the variety of emergent vegetation used in simulation, the user must go to the Riparian Code worksheet and identify the code that represents the desired vegetation type. This value is entered into the white data entry box below the label "Emergent Veg Code". When all input data has been supplied to the white input data cells on the Inputs worksheet, the user then presses the "Reset" command button to prepare the model for a new simulation. The "Run Vegematic" command button fills in the code for the selected vegetation type into the appropriate data input locations on the Main Menu worksheet in order to represent vegetation for the first distance step. These values are automatically copied down to all distance steps on the Main Menu. "Vegematic" then reads the vegetation code from the main menu and fills in the appropriate height, density and overhang values into the rest of the Main Menu riparian data locations. The next executable button on the Inputs worksheet takes the user to the Continuous Data worksheet. The location (distance from the upstream boundary) of each continuous data node (the point of weather data collection) must be specified. Wind speed, relative humidity and air temperature must be provided on an hourly basis throughout the simulation period. Simulation begins at midnight on the first day and the continuous weather data record provided must begin at midnight on the first simulation day. Water temperature may be provided at each continuous data node for validation, but is not required. To return to the Inputs worksheet, the user can select the inputs tab, or click on the "Finish and Return to Inputs" command button at the top of the Continuous Data worksheet. The next command button on the Inputs worksheet is the "Input Initial Conditions" button. The required initial conditions are the water temperature values at midnight of the first simulation day for each distance step. When data input is complete, the model methodology is executed by clicking the next button, "Start Simulation".

Heat Source 6.0 was designed as a daily model, accepting continuous data for a single day and reporting one day's simulation results for that day. It has been adapted to accept ongoing continuous data over several days. At the end of a simulation day, the model was originally designed to present only one day's results. The modified model maintains a record of simulated stream temperatures over the period of simulation as well as solar fluxes above and below riparian vegetation over the course of simulation on a fifteen minute basis. Records of output parameters recorded on a fifteen minute basis are located on the "Validation" worksheet. Following is a review of the model equations used in Heat Source 6.0 and discussion of the model adaptations.

Recalling Equation 9.2, the temperature change due to net heat flux from the environment was simplified for a rectangular channel. This simplification does not apply when modeling a trapezoidal channel with defined side slopes. The temperature change due to environmental heat flux is calculated according to:

$$\frac{\partial T}{\partial t} = -V_x \cdot \frac{\partial T}{\partial x} + \frac{\Phi \cdot A_s}{\rho_{water} \cdot c_p \cdot V} \tag{9.49}$$

where ΔT is the change in temperature for a single distance step during the simulation minute (°C), Φ is the net heat energy flux occurring for one minute (cal/m^2), ρ is the density of water (kg/m^3), c_p is the heat capacity of water (cal/kg-°C), A_s is the stream surface area (m^2), and V is the volume of water in the element (m^3). Field observations of shade cast by Sitka willows planted for the purpose of mitigation after watercourse maintenance showed that willows planted on only one bank may, after several growing seasons, provide complete cover for a narrow watercourse. Therefore, modifications were made to Heat Source 6.0 to describe vegetation that provides this extent of overhang and cover.

9.4.3.2 Shortwave Solar Radiation

In the modified model, vegetation that is strictly bank vegetation exists in only in Zone 1, which has a user defined width perpendicular to the water's edge. Zone 1 is the outermost zone, reaching from the bankfull edge onto adjacent land. Overhanging vegetation is that length of vegetation growing in Zone 1 that extends beyond the bankfull edge, over the sloping bank or the water's surface. Zone 0 is the bank of the watercourse, its width is the model calculated distance between the water's edge and the bankfull edge. This width is based on the calculated wetted width and user defined channel side slopes. The first calculation is the average distance from the bankfull mark to the water's edge. This equation assumes that the transverse distances from the water's edge to bankfull are equal on both banks.

$$Transverse_0 = \frac{Bankfull_{Width} - Wetted_{Width}}{2} \tag{9.50}$$

where $Transverse_0$ is the distance from the water's edge to the bankfull edge (meters).

To calculate solar radiation received at the water's surface, the sunward bank is identified using a comparison of defined stream aspect and calculated solar azimuth angles. The length of shadow cast by the sunward bank itself is first approximated:

$$Shadow_{widthBank} = \frac{Incision \cdot \sin\left|\theta_{azimuth} - \theta_{aspect}\right|}{\tan\theta_{sun}} \tag{9.51}$$

where $Incision$ is the vertical distance that the bank extends above the water's surface. The incision distance is a model input that must be measured in the field. The length of shadow cast by the stream bank that exists only on the water's surface is this shadow length minus the transverse distance. If the shadow length minus the transverse distance is greater than the wetted width, the fraction of the water's surface covered by the bank's shadow is set to 1.

After the length of shadow cast by the bank has been determined, the length of shadow cast by vegetation on the sunward bank and by overhanging vegetation growing on the opposite bank are determined. Excluding emergent and overhanging vegetation, riparian vegetation is assumed to exist landward of top of the bank at the bankfull elevation above the water's surface. The distance of riparian vegetation from the water's edge is calculated based on field-measured channel dimensions and calculated wetted width. In fact, mature, woody riparian vegetation

commonly overhangs the channel for a considerable distance over the stream's surface. However if riparian vegetation does not overhang the water's surface, the transverse distance from the water's edge to the leading edge of the riparian vegetation is calculated as follows:

$$Transverse_1 = Transverse_0 - Veg_{Overhang} \quad (9.52)$$

The model has been adapted so that if the overhanging length is greater than the transverse distance $Transverse_0$ to the water's edge, then the vegetation overhangs the water's surface.

$$Overhang_{length} = \left| Transverse_0 - Veg_{Overhang} \right| \quad (9.53)$$

Vegetation existing only on the bank is considered separately from the portion of the vegetation that is overhanging. Because of this distinction, the transverse distance from the water's edge to the leading edge of the bank vegetation is set to the bank transverse distance.

$$Transverse_1 = Transverse_0 \quad (9.54)$$

The length of shadow cast by vegetation on the sunward bank at distance $Transverse_0$ from the water's edge is calculated. The model is adapted so that this shadow length is transformed by the value of the overhang length, to represent the shadow cast from the edge of the overhang based on a formula developed by Chen et al. (1998a).

$$Shadow_{width} = \frac{VegH_{apparent} \cdot \sin\left|\theta_{azimuth} - \theta_{aspect}\right|}{\tan\theta_{sun}} + Overhang_{length} \quad (9.55)$$

As previously described, the shade density of a shadow cast by riparian vegetation is calculated by first estimating a riparian extinction coefficient for the vegetated zone according to the methodology described by Chen et al. (1998a). If the length of the shadow cast by riparian vegetation on the sunward bank is greater than the transverse distance and also greater than the shadow cast by the bank, then a fraction of the streams surface is shaded only by vegetation. Heat Source 6.0 methodology is adapted so that the shadow from vegetation on the sunward bank may overlap with the shadow cast by overhanging vegetation on the opposite bank. The shadow cast by overhang from the non-sunward bank begins at the sunward edge of overhanging vegetation, over the water's surface. The shadow will be cast toward the non-sunward bank from the position of the leading edge of overhang over the water's surface. The length of a shadow cast by overhanging vegetation on the opposite bank is approximated as:

$$Shadow_{OverhangOpposite} = OverhangLength - \frac{Incision \cdot \sin\left(\theta_{azimuth} - \theta_{aspect}\right)}{\tan\left(\theta_{solar}\right)} \quad (9.56)$$

The length of this shadow over the water's surface is the shadow length minus the transverse distance to bankfull, which is included in the overhang length. The shadow density cast by

vegetation is a function of the density of vegetation and the path length through vegetation as described by Chen et al. (1998a).

$$\lambda = -\frac{Ln\left(1 - VegDensity\right)}{VegH_{actual}} \tag{9.57}$$

where λ is the riparian extinction coefficient (m^{-1}), VegDensity is typically estimated from aerial photographs as the percentage of land in the riparian zone occupied by vegetation (dimensionless), $VegH_{actual}$: Height of riparian vegetation (meters), Veg_{width} is the width of vegetation from bankfull edge perpendicular to the bank (meters), and PL_{veg} is the approximated path length of solar radiation through riparian vegetation (meters).

The path length approximation follows methods outlined by Boyd and Kasper (2003) for riparian and emergent vegetation. Before the sun's altitude angle reaches the top of riparian vegetation:

$$PL_{veg} = \frac{Veg_{width} + Veg_{overhang}}{\left|\sin\left|\theta_{azimuth} - \theta_{aspect}\right|\right| \cdot \cos\theta_{sun}} \tag{9.58}$$

When the sun is overhead of overhanging or emergent vegetation:

$$PL_{vegOver} = \frac{Veg_{height}}{\sin\theta_{sun}} \tag{9.59}$$

The density of the shadow cast by vegetation is determined based on Beer's Law according to Chen et al. (1998a):

$$Shadow_{density} = 1 - e^{-\lambda \cdot PL_{veg}} \tag{9.60}$$

The water's surface may be shaded by the sunward bank's vegetation only, both banks' vegetation at once, the sunward bank itself, or overhanging vegetation from the opposite bank only. The fraction of the water's surface shaded by the bank receives no solar radiation, in a manner similar to that described by Boyd and Kasper (2003). Solar radiation received by the fraction of the water's surface shaded by vegetation is determined as follows:

$$\Phi_{shadedVegetation} = \Phi_{SRA} \cdot \alpha_{shadedSunward} \cdot \left(1 - Shadow_{densitySunward}\right) \tag{9.61}$$

$$\Phi_{shadedOverhang} = \Phi_{SRA} \cdot \alpha_{shadedOverhang} \cdot \left(1 - Shadow_{densityOverhang}\right) \tag{9.62}$$

The shadow from vegetation on the sunward bank may overlap with the shadow cast by overhanging vegetation on the opposite bank. Solar radiation reaching the fraction of the surface shaded by overlapping shadows is calculated as:

$$\Phi_{shadedOverlap} = \Phi_{SRA} \cdot \alpha_{shadedOverlap} \cdot (1 - Shadow_{densitySunward}) \cdot (1 - Shadow_{DensityOverhang}) \quad (9.63)$$

The total solar flux reaching the shaded fraction of the wetted width is the sum of solar radiation through bank vegetation, overhanging vegetation, and the overlap of shadows from both.

$$\Phi_{shadedFraction} = \Phi_{shadedOverlap} + \Phi_{shadedVegetation} + \Phi_{shadedOverhang} \quad (9.64)$$

Solar radiation on the unshaded fraction of the stream's surface is calculated as:

$$\Phi_{unshadedFraction} = \Phi_{SRA} \cdot (1 - \alpha_{shaded}) \quad (9.65)$$

Where the total fraction shaded is the sum of the fractions shaded by the bank, the sunward vegetation only, overhanging vegetation from the opposite bank only, and the fraction shaded by vegetation from both banks at once.

Direct beam shortwave solar radiation routed to the stream surface is calculated as the sum of the solar radiation flux received by the shaded and unshaded fractions of the water's surface.

$$\Phi_{SRV} = \Phi_{shadedFraction} + \Phi_{unshadedFraction} \quad (9.66)$$

Where emergent reed canarygrass is present, direct beam shortwave solar radiation is next routed through this particular type of emergent vegetation. Emergent vegetation is assumed to be of uniform density across the water's surface. The shade density for emergent vegetation is estimated according to the same relationships used for bank vegetation, and the path length is estimated according to the same relationship described for bank vegetation when the sun is overhead as presented by Boyd and Kasper (2003).

The total of Direct and Diffuse Solar Radiation passing water's surface is:

$$\Phi_{TDS} = \Phi_{SRW} + \Phi_{SDVO2} \quad (9.67)$$

The Net Solar Radiation Flux is:

$$\Phi_{solar} = \Phi_{SRW} + \Phi_{DRW} - \Phi_{absorbed} = \Phi_{TDS} - \Phi_{absorbed} = \Phi_{TDS} \quad (9.68)$$

9.4.3.3 Long Wave (Thermal)

Recall that emitted long-wave solar radiation reaching the water's surface is a function of canopy closure over the stream. Modifications have been made to the determination of canopy closure or open sky view (View_To_Sky) to best represent extensively overhanging vegetation. The open sky view is determined as the sum of open sky view for the right and left banks. To determine the fraction of a 90° field of view that is unobstructed, in the modified model a check is made to

determine if overhanging vegetation extends beyond the mid point of the wetted width from either bank.

If vegetation from neither bank extends beyond the channel mid-point, then the view to sky for each half of the channel cross-section is calculated as:

$$VTS_{Bank} = \frac{180}{\pi} \cdot \tan^{-1}\left(\frac{VHeight_{apparent}}{\frac{WWidth}{2} - OverhangLength} \right) \quad (9.69)$$

The open sky view is zero in the case of complete overhang from both banks. If overhanging vegetation on one bank extends beyond the mid-point of the channel, then one bank's open sky view is zero, and the other is calculated as follows:

$$VTS_{BankS} = 90 - \frac{180}{\pi} \cdot \tan^{-1}\left(\frac{VHeight_{apparentS}}{OverhangLengthS - \frac{WWidth}{2}} \right)$$

$$- \frac{180}{\pi} \cdot \tan^{-1}\left(\frac{VHeight_{apparent}}{\frac{WWidth}{2} - OverhangLength} \right) \quad (9.70)$$

The fraction of a 180° field of view that is open to the sky is calculated as follows presented by Boyd and Kasper (2003):

$$View\_To\_Sky = \frac{VTS_{Bank1} + VTS_{Bank2}}{180} \quad (9.71)$$

Long-wave radiation reaching the water's surface is calculated as the sum of radiation through the canopy opening, and through streamside vegetation calculated separately. Long-wave radiation through the canopy opening is described by:

$$\Phi_{longwaveVegO} = View\_To\_Sky \cdot \Phi_{LongwaveATM} \quad (9.72)$$

Long-wave radiation emitted by riparian vegetation as presented by Boyd and Kasper (2003) is:

$$\Phi_{longwaveVeg} = 0.96 \cdot (1 - View\_To\_Sky) \cdot 0.96 \cdot \sigma \cdot (T_{air} + 273.2)^4 \quad (9.73)$$

Because the stream bank itself may restrict the open sky view when the channel is incised, the modified model subtracts the bank angle from (1-View_To_Sky) when calculating long-wave radiation emitted by riparian vegetation.

$$\Phi_{longwaveVeg} = 0.96 \cdot \left(1 - View\_To\_Sky - BAngle\right) \cdot 0.96 \cdot \sigma \cdot \left(T_{air} + 273.2\right)^4 \quad (9.74)$$

$$BAngle = \left(\frac{2}{\pi}\right) \cdot a\tan\left(\frac{Incision}{\left(\frac{1}{2} \cdot Wwidth\right) + Transverse_0}\right) \quad (9.75)$$

The total atmospheric long wave radiation flux at the water's surface is calculated as the sum of long wave radiation through vegetation and the canopy opening.

$$\Phi_{longwave(+)} = \Phi_{longwaveVeg} + \Phi_{longwaveVegO} \quad (9.76)$$

Net long wave radiation balance at the water's surface is the sum of long wave radiation received by the atmosphere and long wave radiation emitted by the stream.

$$\Phi_{longwave} = \Phi_{longwave(+)} + \Phi_{longwave(-)} \quad (9.77)$$

9.4.3.4 Stream Bed Conduction

Heat Source Version 6 methodology includes an energy balance on the stream bed, where the fraction of the stream bed composed of bedrock may absorb solar radiation routed through the water column. A fraction of this absorbed energy may be transferred back to the water column. According to the Heat Source 6.0 methodology, because the low gradient streambeds under consideration are typically composed entirely of fine organic material and silt, energy storage by the stream bed would be neglected. The modified model replaces this methodology with methods based on the upgraded bed conduction methods used in Heat Source Version 7.0. Soil temperatures are generally cooler and more stable than air or water temperatures. Conduction between the bed and water column is calculated based on the characteristics of the conducting layer according to the fractions of sediment and water that compose the bed. The following equations are according to Boyd and Kasper (2003):

$$\rho_{bed} = \rho_{seidment} \cdot \alpha_{sediment} + \rho_{water} \cdot \alpha_{water} \quad (9.78)$$

$$\nu_{Hyporeic} = P_{wetted} \cdot D_{sediment} \cdot dx \quad (9.79)$$

$$\nu_{water} = \vartheta_{sediment} \cdot P_{wetted} \cdot D_{sediment} \cdot dx \quad (9.80)$$

$$\nu_{sediment} = \left(1 - \vartheta_{sediment}\right) \cdot P_{wetted} \cdot D_{sediment} \cdot dx \quad (9.81)$$

$$\alpha_{sediment} = \frac{\nu_{sediment}}{\nu_{Hyporeic}} \tag{9.82}$$

$$\alpha_{water} = 1 - \alpha_{sediment} \tag{9.83}$$

$$K_{bed} = K_{sediment} \cdot \alpha_{sediment} + K_{water} \cdot \alpha_{water} \tag{9.84}$$

$$\Psi = \Psi_{sediment} \cdot \alpha_{sediment} + \Psi_{water} \cdot \alpha_{water} \tag{9.85}$$

where ρ_{bed} is the volumetric weighted density (kg/m^3), $\rho_{seidment}$ is the substrate density (typically assumed to be 1600kg/m^3), ρ_{water} is the density of water (kg/m^3), α_{water} is the water volume ratio (dimensionless), $\alpha_{sediment}$ is the sediment volume ratio (dimensionless), $D_{sediment}$ is the depth of the conduction layer (m), K_{water} is the water thermal conductivity (typically assumed to be 0.60 J/ m s °C), $K_{sediment}$ is the sediment thermal conductivity (typically assumed to be 15.98 J/ m s °C), K_{bed} is the volumetric composite thermal conductivity in conduction layer (J/ m s °C), ν_{water} is the water volume in conduction layer (m^3), $\nu_{sediment}$ is the substrate volume in conduction layer (m^3), $\nu_{Hyporeic}$ is the total volume in conduction layer (m^3), $\vartheta_{sediment}$ is the porosity of the conduction layer (dimensionless), $\Psi_{sediment}$ is the substrate thermal diffusivity (m^2/s) and Ψ_{water} is the water thermal diffusivity (m^2/s).

The heat flux transferred to the water column is calculated:

$$\Phi_{conduction} = \frac{\Psi \cdot \rho_{bed} \cdot K_{bed} \cdot (T_{Sediment} - T_{water0})}{\frac{D_{sediment}}{2}} \cdot C_{onversionFactor} \tag{9.86}$$

$$\Phi_{sediment} = -\Phi_{conduction} \tag{9.87}$$

$$\Delta T_{sediment} = \frac{\Phi_{sediment} \cdot P_{wetted} \cdot dx \cdot dt}{\rho_{bed} \cdot K_{bed}} \tag{9.88}$$

$$\Delta T_{sediment} = T_{Sediment} + \Delta T_{sediment} \tag{9.89}$$

9.4.3.5 Flow Model

The modified flow model uses Manning's equation to estimate channel flows and velocities. Channel side slope is an important design parameter that impacts bank and riparian vegetation shade. User inputs include water depth, channel bottom width, channel side slope, channel gradient, and Manning's n. The wetland Manning's flow model presented by Crites and Tchobanoglous (1998) has been added to the adapted model as an available option to model flow in watercourses heavily obstructed with vegetation. A general diagram illustrating cross-section parameters used in the Manning flow model is shown in Figure 9-7. Figure 9-7 presents the parameters used to calculate open channel flow for both unobstructed and wetland or obstructed conditions.

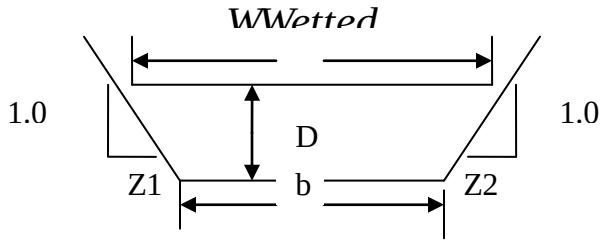

Figure 9-7. Water column and channel cross-section dimensions for Manning's flow model

Unobstructed flow is modeled as follows:

$$Q = V_x \cdot A_c \tag{9.90}$$

where V_x is the flow velocity (meters/second)

$$V_x = \frac{\delta}{n} \cdot R^{2/3} \cdot S^{1/2} \tag{9.91}$$

where R is the hydraulic radius (meters), S is the channel gradient (dimensionless), Q is the discharge (m^3/second), n is Manning's roughness coefficient, A_c is the channel cross-sectional area (m^2), and δ is the conversion factor equal to 1 for metric units

For a trapezoidal channel, R and A_c are calculated as follows:

$$R = \frac{A_C}{P_{wetted}} \tag{9.92}$$

$$A_c = \frac{D}{2} \cdot (b + WWetted) \tag{9.93}$$

where D is the water depth (meters), b is the channel bottom width (meters), and $WWetted$ is the water surface width (meters). For a trapezoidal channel:

$$WWetted = b + D \cdot (Z1 + Z2) \tag{9.94}$$

and P_{wetted} is the wetted perimeter (meters):

$$P_{wetted} = b + D \cdot \left(\sqrt{1 + Z1^2} + \sqrt{1 + Z2^2}\right) \tag{9.95}$$

For wetlands, or obstructed flows, a similar equation applies with an adjustment to n according to Crites et al. (1988):

$$n = \frac{a}{D^{1/2}} \tag{9.96}$$

where a is the resistance factor ($s \cdot m^{1/16}$) defined by:

a = 0.487 for sparse vegetation with Y > 1.3 feet
a = 1.949 for moderately dense vegetation and Y = 1 foot
a = 7.795 for very dense vegetation with a litter layer and Y < 1 foot.

In the wetland Manning's flow model presented by Crites and Tchobanoglous (1998), the hydraulic radius is replaced by water depth and velocity is calculated according to Equation 9.91.

9.5 RESULTS

9.5.1 Model Validation

The modified version of Heat Source 6.0 was validated at four sites representing three vegetation types: 1 Willow site, 2 reed canarygrass sites, and 1 site with no vegetation. Efforts were made to study simplified reaches during low flow conditions when ground water and intermittent variable surface flows would be minimized. Figure 9-8 shows hourly predicted and measured temperature at the downstream end of a site 100 meters in length densely vegetated with willows extending over the entire width of the channel. Simulation results for the five day temperature validation simulation resulted in R^2= 0.77, Root mean square error (RMSE) = 0.41. Results for 14 day simulation at the same site resulted in R^2= 0.87, RMSE = 0.63. Figure 9-8 shows hourly predicted and measured temperature at the downstream end of the reach. Figure 9-8 indicates that predicted and measured temperatures in this validation scenario typically differ by less than half a degree.

Figure 9-9 shows simulated and measured downstream temperatures over a 200 meter reach with dense stands of reed canarygrass on both banks and reed canarygrass growing profusely within the channel. R^2= 0.83 for this simulation and RMSE= 0.17. The modified wetland Manning's flow feature in the adapted model was used for this simulation. Measured and predicted temperatures for this validation simulation typically differ by less than half a degree.

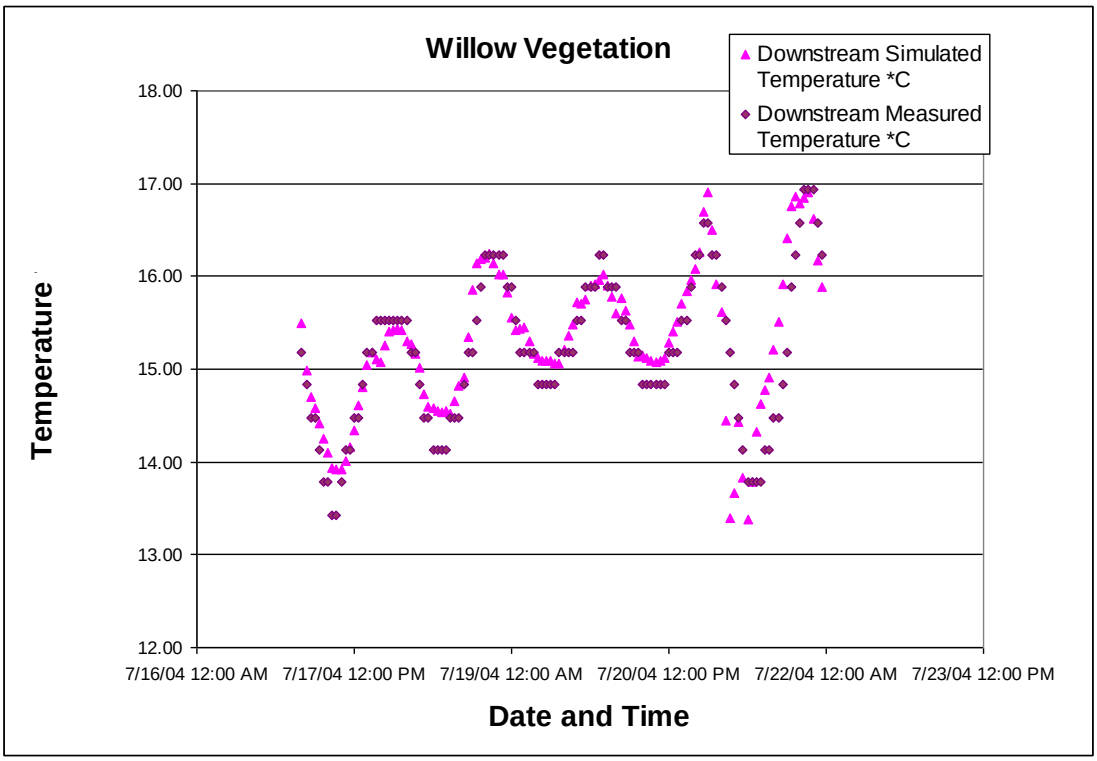

Figure 9-8. Validation results for the modified Heat Source model with willow vegetation

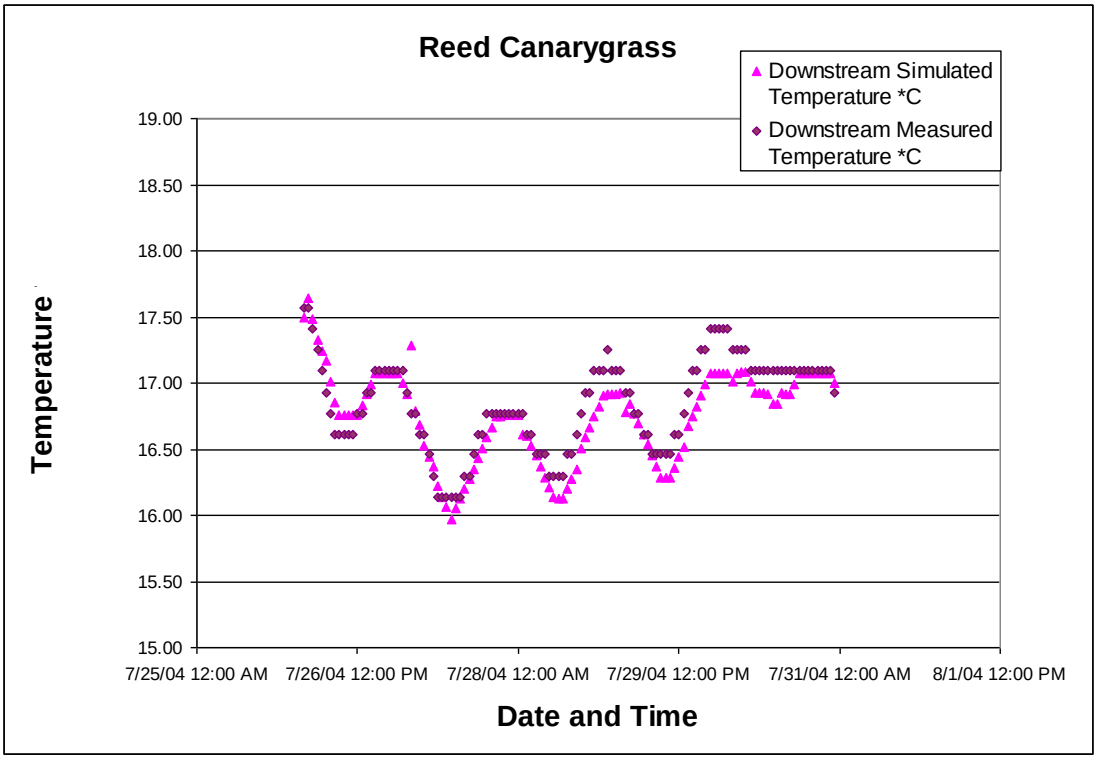

Figure 9-9. Validation results for the modified Heat Source model with reed canarygrass vegetation

Simulation results for a 100 meter reach that was cleared of vegetation during maintenance are presented in Figure 9-10. Results for this simulation showed a $R^2 = 0.76$ and a RMSE= 0.68. Measured and predicted temperatures in this validation scenario also typically differ by less than half a degree.

Temperature validation results from simulation over a 360 meters reach with dense stands of reed canarygrass on both banks and reed canarygrass growing profusely within the channel are presented in Figure 9-11. This simulation shows greater error compared with results from other validation simulations. This error can be seen in the difference between simulated and measured temperatures, for example close to 12:00 July 17th. Simulation results showed $R^2 = 0.77$, RMSE= 0.65. Although no net change in flow could be measured across this reach, potential sources of model error include un-detected ground water exchange. A small ephemeral tributary to this reach was observed to have zero flow during the validation period, but could have had an undetected subsurface component.

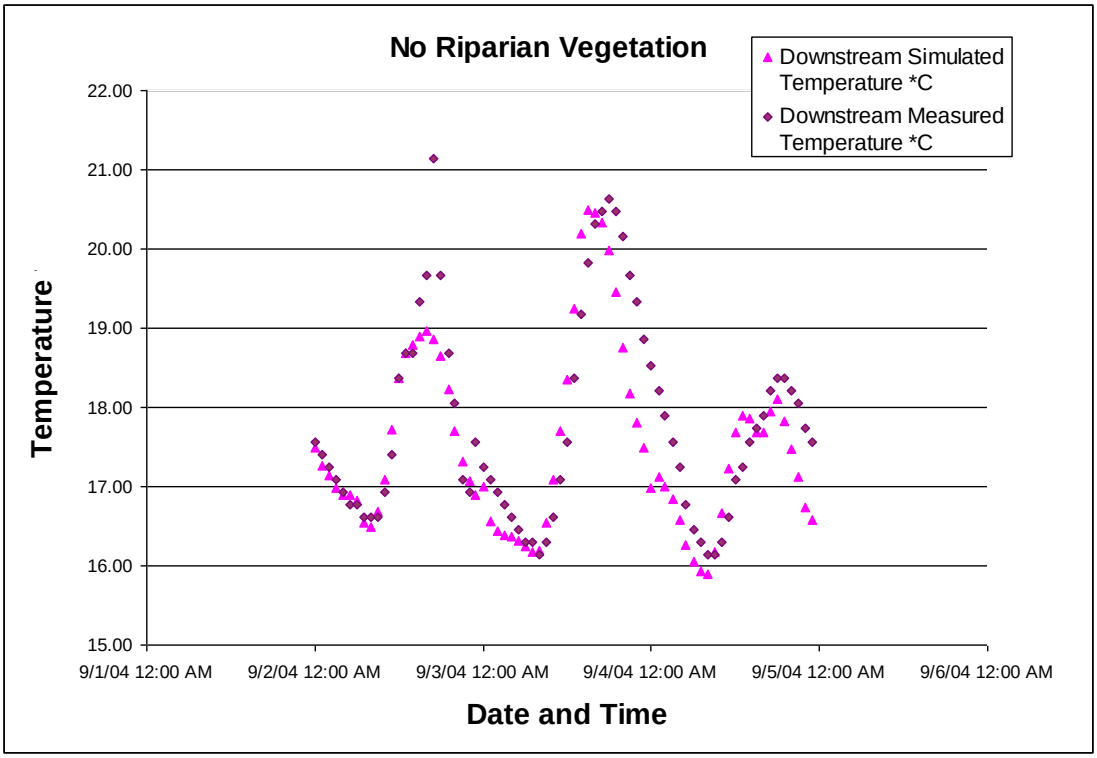

Figure 9-10. Validation results for the modified Heat Source model with no riparian vegetation

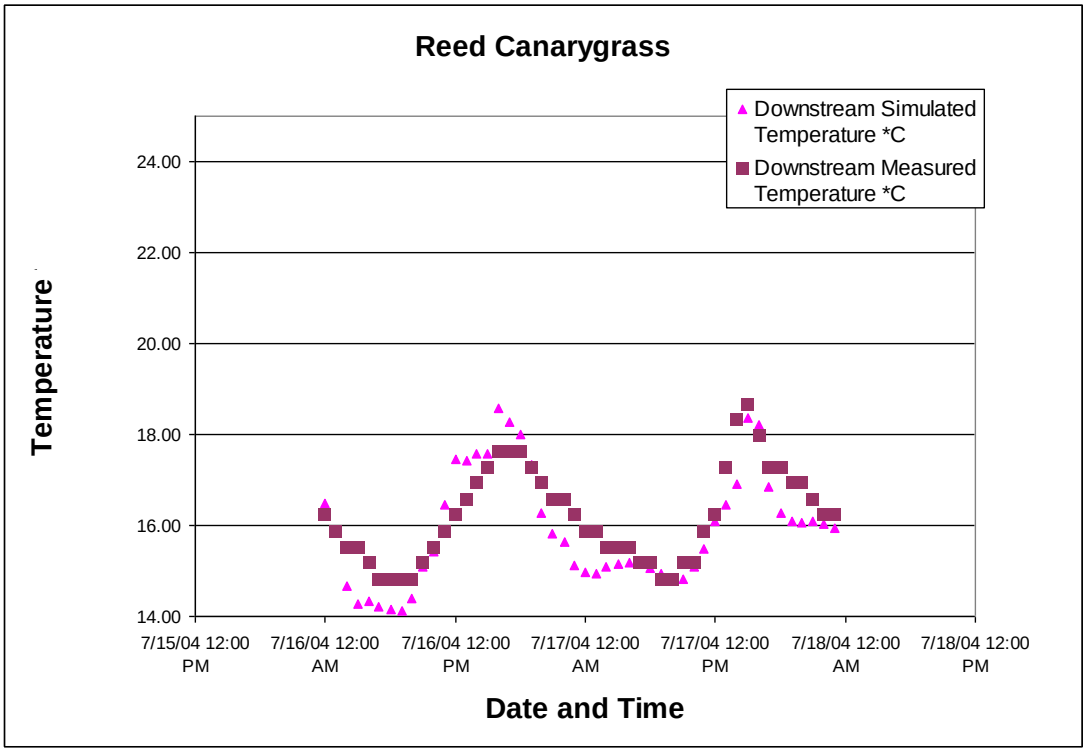

Figure 9-11. Validation results for the modified Heat Source model with reed canarygrass vegetation

While error is observable in these validation simulations, it is generally less than half a degree. The willow vegetation validation scenario appears to show more error at low temperatures, while Figure 9-9, validation for reed canarygrass, shows most error during high temperatures. Figure 9-10 shows a small amount of temporal offset, indicating that the simulated time of travel may be slower than the actual. No consistent type of error is evident in these validation simulations and error is generally small.

9.5.2 Sensitivity Analysis of Major Design and Management Parameters

The objective of sensitivity analysis is to identify the magnitude of the model's response to individual input data parameters over the practical range of input values. Sensitivity analysis is used to determine the factors that have the greatest effect on system response. The model's response to a change in each input parameter is found by comparing each "test" scenario result with the one "baseline" scenario result. Because model sensitivity may depend on baseline conditions, two baseline scenarios are considered to evaluate model sensitivity over the range of reasonable input values.

Sensitivity analysis is carried out by changing the value of exactly one parameter at a time. For this reason, sensitivity scenarios do not necessarily yield scenario results that are practical from a management perspective. Sensitivity analysis results should not be confused with maintenance scenarios. For example, in a real world scenario, watercourse morphology may be altered to result in decreased watercourse depth, yet the flow in the channel may remain constant, since other watercourse characteristics would have also changed to accommodate the same flow. In a sensitivity analysis scenario, decreasing only watercourse depth results in a smaller calculated flow. Sensitivity analysis results do not necessarily represent the change in temperature that would occur as changes are made to one watercourse, they indicate the sensitivity of the model to input parameters.

Table 9-1 outlines the input parameters used for baseline 1 in the sensitivity analysis conducted during this project. The RCG density used for this sensitivity analysis was set at 93%. This value was selected to make the shadow cast by reed canarygrass at least slightly different from the shadow that would be cast by an opaque object in order to derive a conservative estimate of the sensitivity of the model to shade produced by reed canarygrass. The width of buffer vegetation on the bank was defined at 2.5 meters. In most observed field conditions, all types of riparian vegetation were at least this wide.

Weather data used in simulation was gathered from the University of Washington rooftop weather station. Online one-minute data is available for download at:
http://www-k12.atmos.washington.edu/k12/grayskies/nw_weather.html

Table 9-1. Baseline 1 parameters for sensitivity analysis

Parameter	Base Line Value	Units
Simulation Period	14	days
Start date	7/15/04	
Lat	42.6	degrees
Long	-121.6	degrees
Aspect	180	degrees
Right Side Slope	2	H:V
Left Side Slope	2	H:V
Incision	0.5	meters
Bottom width	2.0	meters
Water Depth	0.15	meters
Manning's n	0.2	
Channel gradient	0.001	%
Right Bank Vegetation	RCG	
Left Bank Vegetation	RCG	
Sediment Depth	0.5	meters
Sediment Temperature	13.7	degrees C

Table 9-2 outlines the results of sensitivity analysis simulations for predicted Maximum 7-Day Average of Daily Maximum Temperatures. Changes in parameters including flow depth and side slope also impact simulated discharge and surface area. Consideration of these impacts is useful in analyzing simulation results. For this reason, descriptive parameters such as effective shade and discharge are included in Table 9-3.

The sensitivity coefficients, determined for each simulation as the ratio of the percentage change in the maximum seven day average of daily maximum temperature divided by the percent change in input parameter, are shown in Table 9-2. Air temperature is the parameter with the highest model sensitivities among all values and parameters tested for this baseline scenario. Air temperature was adjusted by increasing every hourly measured air temperature input value by the number of degrees indicated in Table 9-3.

Table 9-2. Sensitivity coefficients for Baseline 1 modified Heat Source

Parameter	% Change in Parameter	% Change in the Maximum Seven Day Average of Daily Maximum Temperatures	Sensitivity Coefficient
Air Temperature	25.9	0.84	0.326
	-25.9	-0.84	0.326
	51.75	1.69	0.326
Flow Depth	-33.33	3.80	-0.114
	33.33	-0.93	-0.027
	100.00	-0.54	-0.005
	233.33	0.19	0.008
	566.33	0.61	0.011
	6.67	-0.31	-0.04
	100.00	-0.54	-0.005
	13.33	-0.52	-0.039
Incision	-100.00	-3.86	0.039
	-80.00	-2.91	0.036
	100.00	0.22	0.002
	-10.00	-0.04	0.004
	10.00	0.03	0.003
	-20.00	-0.11	0.005
Side Slope	-50.00	-0.49	0.010
	25.00	0.22	0.009
	50.00	0.76	0.015
Effective Shade From Stream Bank	58.16	-3.86	-0.009
	-33.48	-2.91	-0.023
	-19.05	0.22	-0.011
Effective Shade From Vegetation	343.70	-3.62	-0.011
	233.45	-3.31	-0.014
	-68.20	1.01	-0.015
Bottom Width	-50.00	0.12	-0.002
	-25.00	0.38	-0.015
	25.00	-0.20	-0.008
Sediment Depth	-40.00	-1.43	0.036
	40.00	0.98	0.024
	300.00	2.06	0.007

Table 9-3. Baseline 1 Sensitivity Analysis Results Modified Heat Source

Test Parameter	Test Parameter Value	Maximum 7-Day Average of Daily Maximum Temperature °C	Discharge	Flow Velocity	Date and Time of Maximum	Depth	Wetted Width	Effective Shade
Baseline		18.3	0.014	0.04	7/23/04 3:00 PM	0.15	2.6	0.20
Side Slope	1:1	18.2	0.013	0.04	7/23/04 3:00 PM	0.15	2.3	0.32
Side Slope	3:1	18.5	0.015	0.04	7/23/04 3:00 PM	0.15	2.8	0.14
Side Slope	2.5:1	18.4	0.014	0.04	7/23/04 3:00 PM	0.15	2.8	0.16
Willow Density	93%	17.6	0.014	0.04	7/23/04 5:00 PM	0.15	2.6	0.90
Willow Density	50%	17.7	0.014	0.04	7/23/04 5:00 PM	0.15	2.6	0.68
Willow Density	20%	18.3	0.014	0.04	7/23/04 3:00 PM	0.15	2.6	0.20
Bank Incision	1.0	18.3	0.014	0.04	7/23/04 3:00 PM	0.15	2.6	0.19
Bank Incision	0.1	17.7	0.014	0.04	7/23/04 4:00 PM	0.15	2.6	0.77
Bank Incision	0.0	17.6	0.014	0.04	7/23/04 5:00 PM	0.15	2.6	0.70
No Vegetation	0	18.4	0.014	0.04	7/23/04 5:00 PM	0.15	2.6	0.06
Water Depth	0.5	18.3	0.120	0.09	7/23/04 4:00 PM	0.50	3.2	0.14
Water Depth	0.1	18.5	0.007	0.03	7/23/04 2:00 PM	0.10	2.4	0.22
Water Depth	1.0	18.3	0.459	0.12	7/23/04 5:00 PM	1.01	6.0	0.10
Sediment Depth	0.3	18.1	0.014	0.04	7/23/04 3:00 PM	0.15	2.6	0.20
Sediment Depth	0.7	18.4	0.014	0.04	7/23/04 3:00 PM	0.15	2.6	0.20
Sediment Depth	2	18.6	0.014	0.04	7/23/04 3:00 PM	0.15	2.6	0.2
Bottom width	1	18.5	0.0074	0.0378	7/23/04 2:00 PM	0.15	1.6	0.28
Bottom width	1.5	18.3	0.0106	0.0394	7/23/04 3:00 PM	0.15	2.1	0.24
Bottom width	2.5	18.2	0.0173	0.0411	7/23/04 3:00 PM	0.15	3.1	0.18
Air Temperature	Increase 5°C	18.4	0.014	0.040	7/23/04 3:00PM	0.15	2.6	0.20
Air Temperature	Decrease 5°C	18.1	0.014	0.040	7/23/04 3:00PM	0.15	2.6	0.20
Air Temperature	Increase 10°C	18.6	0.014	0.040	7/23/04 3:00PM	0.15	2.6	0.20

9.5.2.1 Flow Depth

Figure 9-12 shows the change in predicted maximum seven day average of daily maximum temperatures versus the change in input depth. As user defined flow depth decreases, the calculated discharge used to model temperature also decreases. The volume of water receiving net-heat exchange is smaller and because of this the system is more dynamic. The maximum seven day average temperature output was similarly sensitive to a change in depth, with sensitivity increasing as depth decreases because increase flow tends to decrease the impact of the heat balance on a reach. If the net flux in a reach is negative, the reach will have less cooling impact on a watercourse with larger flow. If the net flux is positive the watercourse will show less warming if flow is greater. In addition, if increased velocity is the only mechanism responsible for increasing flow, a water element will spend less time within a defined stream reach in the environment and exchange less total energy than an equal, slower moving volume. This is consistent with the relationships and findings of Larson and Larson (1997) and Brown (1969). In a channel with sloping sides, the wetted width that can be exposed to solar radiation increases with increasing depth.

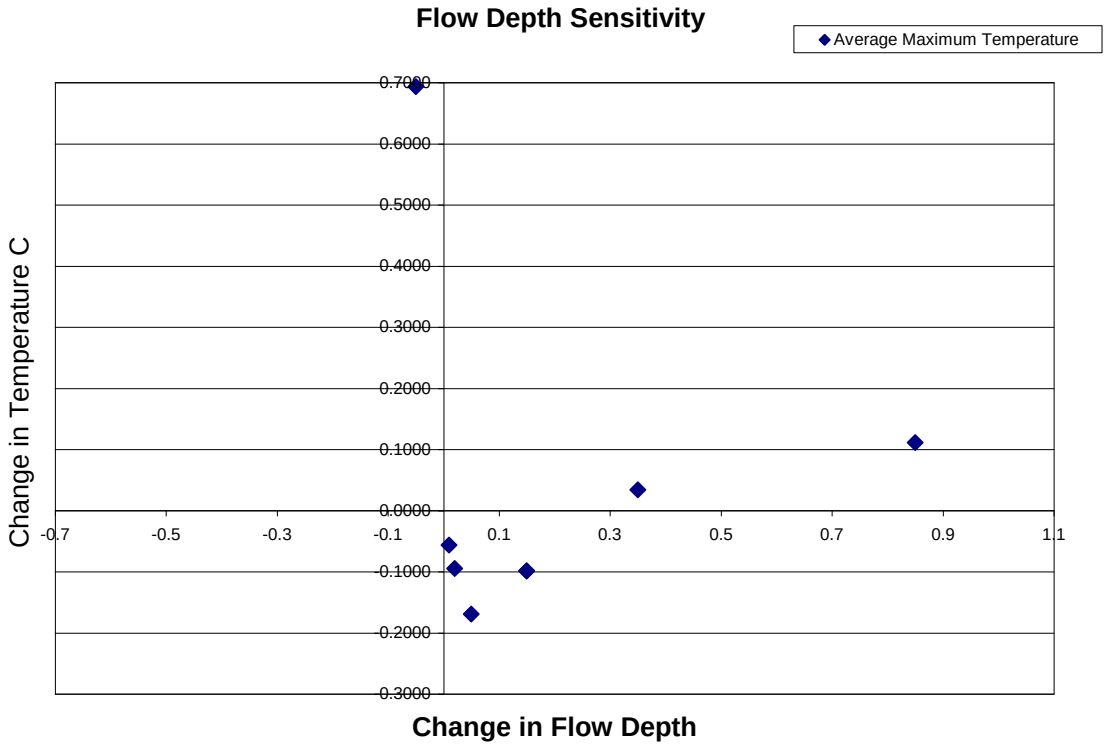

Figure 9-12. Sensitivity of the maximum seven day average of daily maximum temperatures to flow depth

9.5.2.2 Effective Shade

Figure 9-13 shows the change in the predicted maximum seven day average of daily maximum temperatures versus the change in effective shade. Effective shade is the percent reduction in

solar radiation reaching the water's surface. Parameters that reduce the amount of solar radiation that reaches the water's surface include channel morphology such shade-producing channel incision, shade from riparian vegetation, and shade from topographic features. Sensitivity analysis for effective shade was carried out by changing vegetation density, height, width and overhang. The temperature response to change in effective shade is relatively non-linear. The decrease in temperature slows as effective shade increases. This model behavior is reasonable because as the warming influence of solar radiation is reduced, other warming factors, such as air temperature remain un-changed by shade.

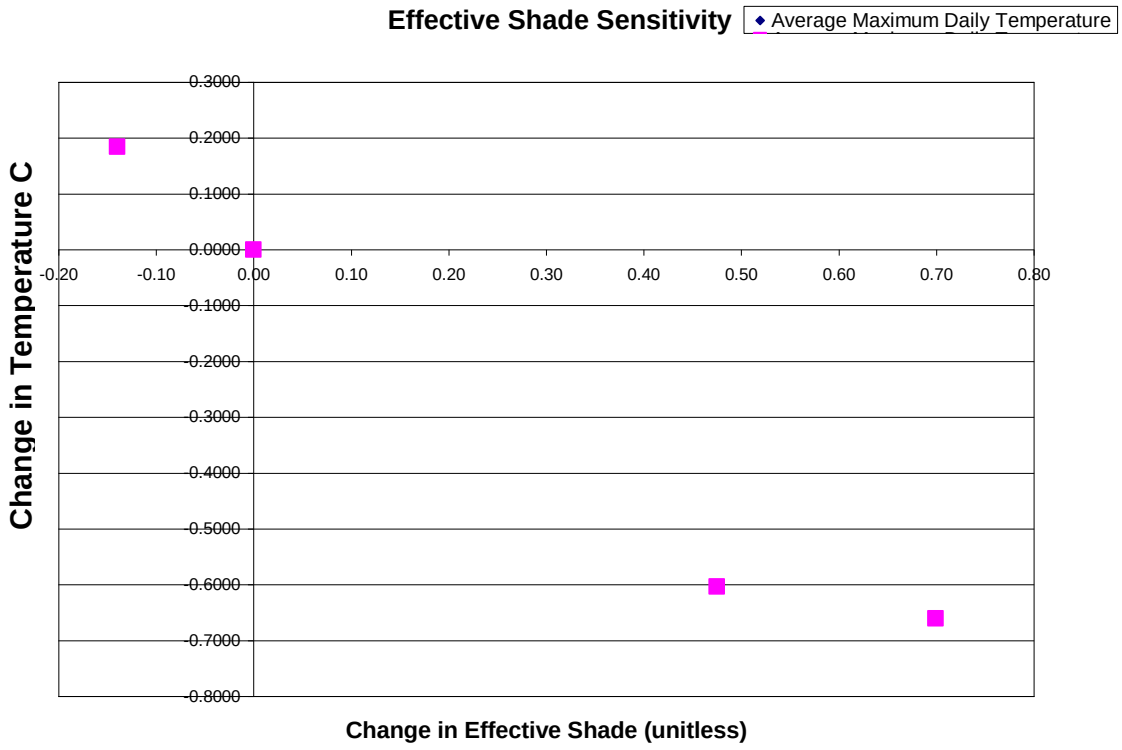

Figure 9-13. Sensitivity of the maximum seven day average of daily maximum temperatures to effective shade

9.5.2.3 Channel Incision

Figure 9-14 shows the change in predicted maximum seven day average of daily maximum temperatures versus change in channel incision. Channel incision may increase or reduce effective shade depending on channel side slope. For the same incision distance, a bank with a shallower side slope will provide less effective shade. Vegetation at the top of a deeply incised long sloping bank will be farther from the water's surface, and therefore must be either taller or extend further over the channel to provide the same shade as the same vegetation growing at the edge of the stream. Vegetation that takes root between the banks is considered either emergent or overhanging. No emergent vegetation is present in this scenario. When the channel banks are steep, riparian vegetation on the bank remains close to the water's edge, but is effectively taller

and able to cast a shadow further thereby providing more effective sky closure of the stream's 180 degree open sky view. The change in temperature with change in incision is also non-linear as is the relationship of temperature to effective shade.

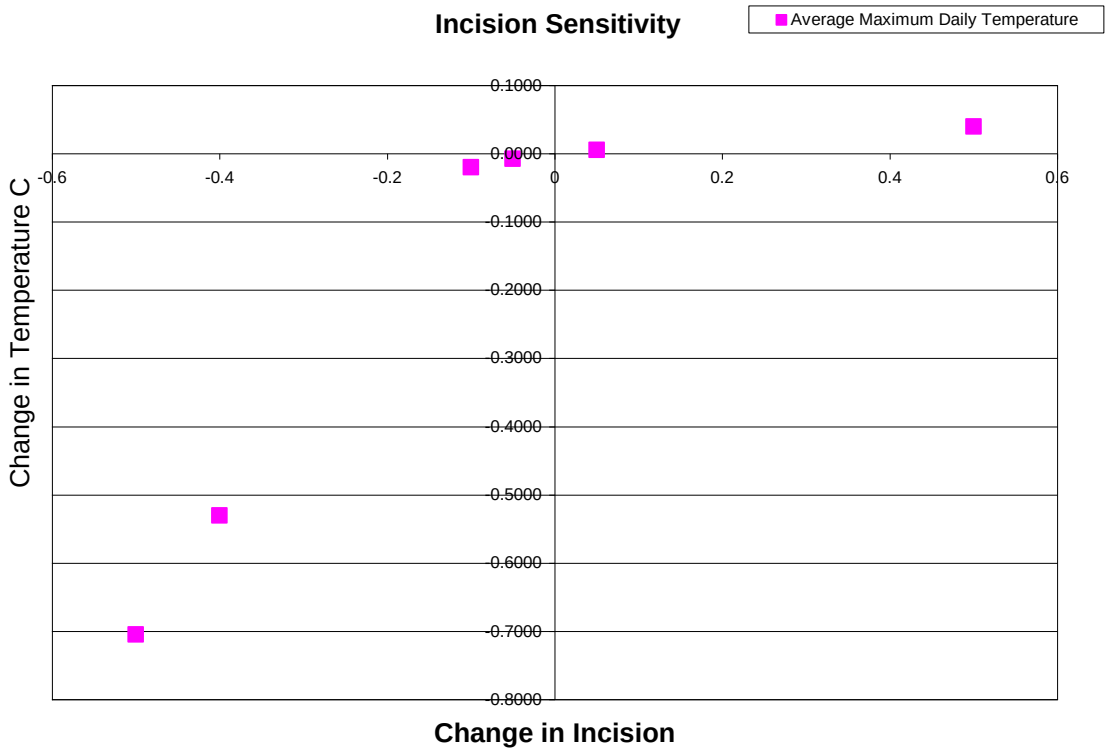

Figure 9-14. Sensitivity of the maximum seven day average of daily maximum temperatures to change in incision depth

9.5.2.4 Bottom Width

Figure 9-15 shows the change in predicted maximum seven day average of daily maximum temperatures with change in bottom width. With a fixed water depth, increasing the bottom width has two effects: it increases simulated flow volume by increasing cross-sectional area and it increases top width and potential surface area available for energy transfer. Of these two parameters an increase in flow volume has a greater influence on energy transfer. Under baseline conditions, effective shade is not greatly influenced by the increase in bottom width, so the increase in solar exposure with increased top width is less important than the effect of increase in volume. The bottom width sensitivity simulations represent increasing flow and decreasing effective shade as the bottom width ranges from 1 to 2.5 meters.

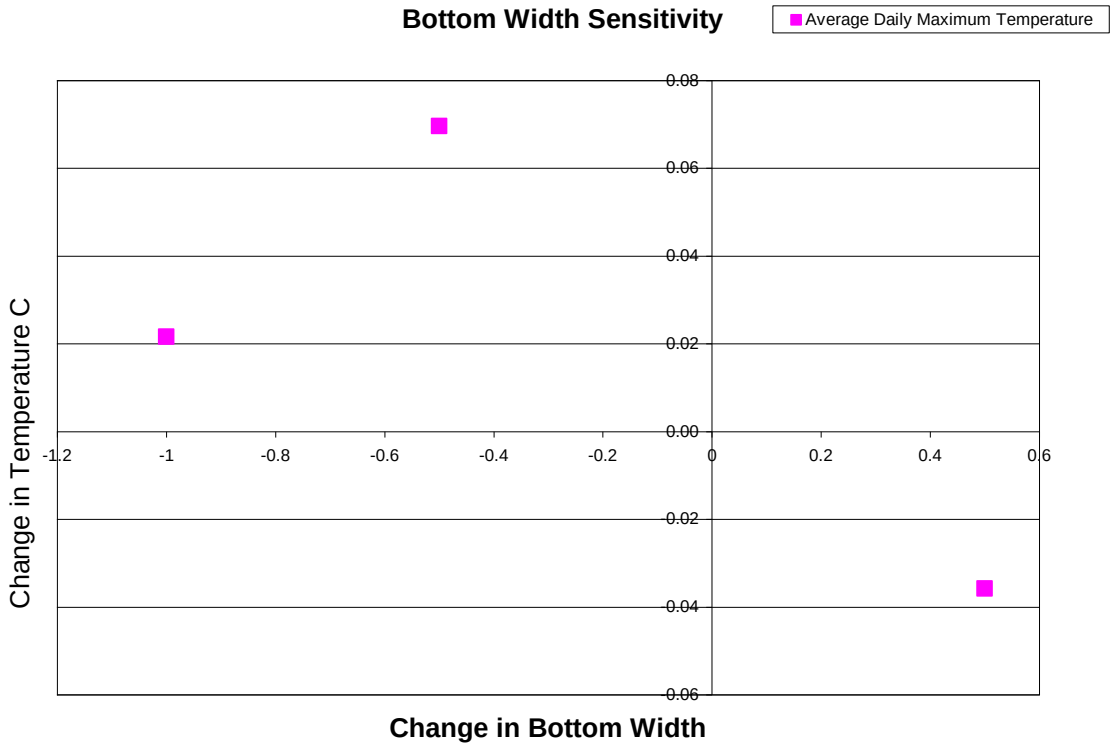

Figure 9-15. Sensitivity of maximum seven day average of daily maximum temperatures to channel bottom width

9.5.2.5 Air Temperature

Figure 9-16 shows the change in predicted maximum seven day average of daily maximum temperatures to change in daily air temperatures. Stream temperature shows a relatively linear relationship with air temperature for this baseline scenario over the range tested. The large slope of the graph of change in water temperature versus change in air temperature indicates high sensitivity. Water temperature has a strong dependence on air temperature for the scenario tested. It is important to remember that the only variable changed in this sensitivity scenario is hourly air temperature. In a realistic scenario, increased air temperatures would also increase the model's upstream temperature boundary condition. This change could result in a greater overall temperature change in response to change in air temperature.

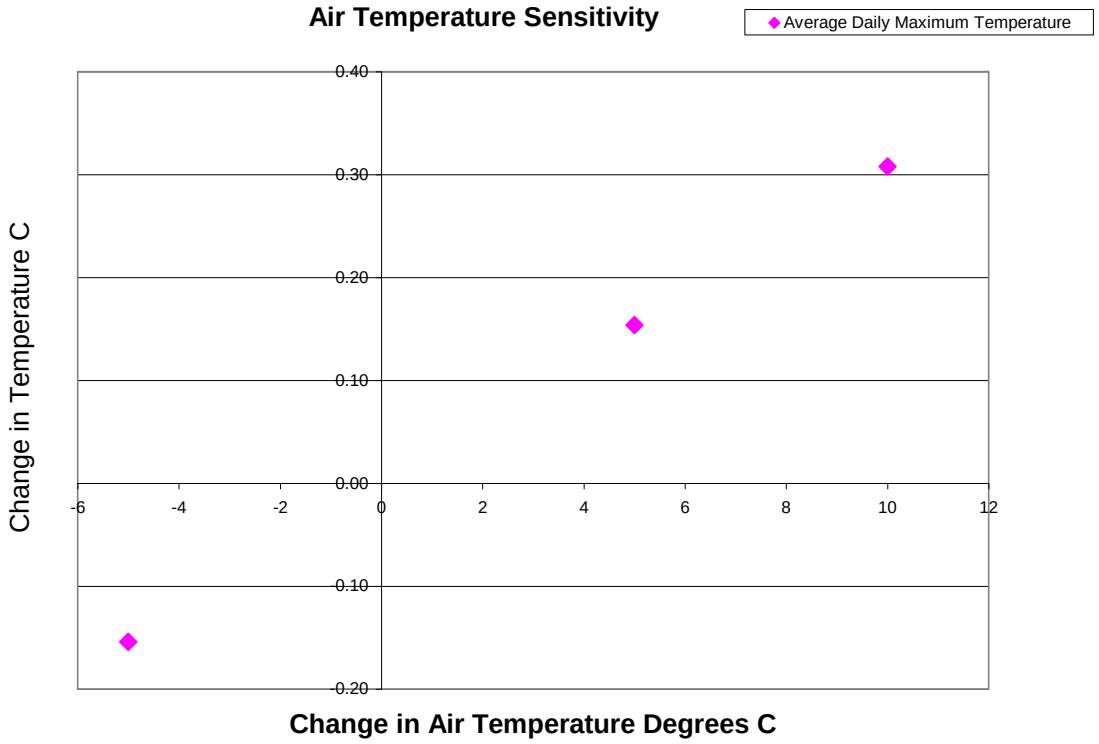

Figure 9-16. Sensitivity of maximum seven day average of daily maximum temperatures to air temperature

9.5.2.6 Sediment Depth

Figure 9-17 shows the change in predicted maximum seven day average of daily maximum temperatures with change in channel sediment depth. Recall that the sensitivity coefficient is equal to the percent change in temperature divided by the percent change in input parameter. The results shown in Figure 9-17 indicate that decreasing the sediment depth initially has a significant impact on the predicted temperature. Conversely, increasing sediment depth significantly has a diminishing rate of influence. However, the model assumes that the conducting sediment is similar in density to soil which may not be thoroughly descriptive of the fine-grained, low density material -- much of it organic -- that actually accumulates rapidly on the bottom of flat gradient slow-moving watercourses that obstructed by profuse growths of reed canarygrass.

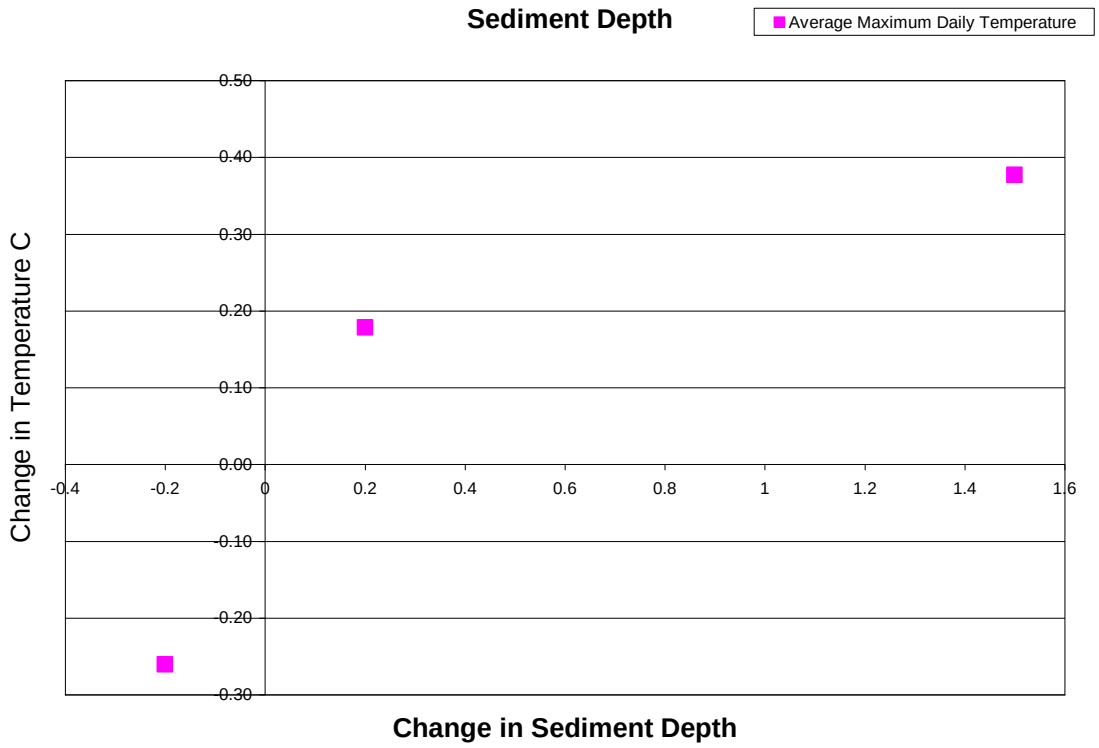

Figure 9-17. Sensitivity of seven day average of daily maximum temperatures to sediment depth

9.5.2.7 Impact of Channel Morphology on Effective Shade

One difficulty in obtaining representative sensitivity analysis results is that the model's sensitivity to a specific input parameter may change with different values of the same input parameter. Sensitivity also may depend on assumed conditions. For example, the sensitivity of stream temperature to the shade of vegetation may be greater when no bank shade is present. When the bank significantly shades the watercourse, water temperature may not respond to additional shade from vegetation. These assumed conditions, such as stream bank shading, are part of the "baseline" scenario. The baseline scenario is a set of input data used for repeated comparison with simulation results as input values are varied one at a time.

The sensitivity of the stream system's response to solar radiation and effective shade depends on the channel size and morphology. The second baseline condition used to identify potential sensitivity to effective shade is a channel with vertical side slopes. This channel form was selected in order to test the effect of very steep slopes on water temperature. In using vertical slopes as input parameters, it should be noted that such slope are inherently unstable and not likely to be encounted under actual field conditions. Still, considering vertical side slopes gives an idea of temperature sensitivities in the extreme case when side slopes are very steep. The input parameters used for baseline 2 are described in the Table 9-4.

Table 9-4. Sensitivity analysis input parameters for Baseline 2 modified Heat Source

Parameter	Baseline Value	Units
Simulation Period	14	days
Start date	7/15/04	
Lat	42.6	degrees
Long	-121.6	degrees
Aspect	180	degrees
Right Side Slope	0.001	H:V
Left Side Slope	0.001	H:V
Incision	0.5	meters
Bottom width	1.5	meters
Water Depth	0.15	meters
Manning's n	0.2	
Channel gradient	0.001	
Right Bank Vegetation	RCG	
Left Bank Vegetation	RCG	
Sediment Depth	0.5	meters
Sediment Temperature	13.7	degrees C

Table 9-5 shows the detailed results for the sensitivity analysis using baseline scenario 2. As each parameter is varied in the sensitivity analysis using baseline 2, it influences the value of other parameters. Consideration of the values of other parameters as presented in Table 9-5, aids in analysis and explanation of sensitivity analysis results.

Table 9-6 presents sensitivity analysis results for baseline scenario 2. The sensitivity of this baseline scenario to air temperature shade is much smaller than the sensitivity of baseline 1 to air temperature, while the sensitivity of effective shade is greater.

Table 9-5. Sensitivity analysis results for Baseline scenario 2

Test Parameter	Test Parameter Value	Maximum 7-Day Average of Daily Maximum Temperature °C	Discharge	Flow Velocity	Date and Time of Maximum	Depth	Wetted Width	Effective Shade
Baseline		17.9	0.009	0.04	7/23/04 5:00 PM	0.15	1.5	0.80
Air Temperature	Increase 5°C	18.1	0.009	0.04	7/23/04 5:00 PM	0.15	1.5	0.80
Air Temperature	Decrease 5°C	17.8	0.009	0.04	7/23/04 5:00 PM	0.15	1.5	0.80
Air Temperature	Increase 10°C	18.2	0.009	0.04	7/23/04 5:00 PM	0.15	1.5	0.80
Flow Depth	0.3	18.2	0.03	0.06	7/23/04 5:00 PM	0.3	1.5	0.80
Flow Depth	0.25	18.2	0.02	0.05	7/23/04 5:00 PM	0.25	1.5	0.80
Flow Depth	0.13	17.9	0.01	0.04	7/23/04 3:00 PM	0.13	1.5	0.80
Flow Depth	0.1	17.9	0.01	0.03	7/23/04 3:00 PM	0.10	1.5	0.80
Bank Incision	0.1	17.9	0.008	0.04	7/23/04 4:00 PM	0.15	1.5	0.76
Bank Incision	1.0	17.9	0.008	0.04	7/23/04 4:00 PM	0.15	1.5	0.83
Bank Incision	0.7	17.9	0.008	0.04	7/23/04 4:00 PM	0.15	1.5	0.82
No Vegetation	0.21	18.4	0.008	0.04	7/23/04 4:00 PM	0.15	1.5	0.21
Willows	0.99	17.5	0.008	0.04	7/23/04 5:00 PM	0.15	1.5	0.99
Willows (50%)	0.84	17.6	0.008	0.04	7/23/04 5:00 PM	0.15	1.5	0.84
Bottom Width	0.5	17.4	0.002	0.033	7/23/04 6:00 PM	0.15	1.5	0.96
Bottom Width	0.2	18.0	0.012	0.041	7/23/04 5:00 PM	0.15	1.5	0.76
Bottom Width	1.0	17.9	0.005	0.037	7/23/04 5:00 PM	0.15	1.5	0.87
Sediment Depth	0.7	18.1	0.008	0.04	7/23/04 5:00 PM	0.15	1.5	0.80
Sediment Depth	0.3	17.7	0.008	0.04	7/23/04 5:00 PM	0.15	1.5	0.80
Sediment Depth	2.5	17.5	0.008	0.04	7/23/04 5:00 PM	0.15	1.5	0.80

Table 9-6. Sensitivity coefficients for Baseline 2 sensitivity analysis results from the modified Heat Source model

Parameter	% Change in Parameter	% Change in the Maximum Seven Day Average of Daily Maximum Temperatures	Sensitivity Coefficient
Air Temperature	25.87	0.71	0.027
	-25.87	-0.70	0.027
	51.75	1.42	0.027
Flow Depth	66.67	0.87	0.013
	-13.33	-0.31	0.023
	-33.33	-0.48	0.014
Incision	-80.00	0.00	0.000
	100.00	0.00	0.000
	40.00	0.00	0.000
Effective Shade From Vegetation	-73.41	2.25	-0.031
	24.63	-2.39	-0.100
	5.36	-2.28	-0.430
Bottom Width	-66.67	-3.23	0.049
	33.33	0.04	0.001
	-33.33	-0.08	0.003
Sediment Depth	40.00	0.80	0.012
	-40.00	-1.74	0.044
	-50.00	-2.56	0.051

9.5.2.8 Effective Shade from Vegetation

Sensitivity results obtained using baseline 2 conditions are outlined in Table 9-5. Effective shade was tested by changing the density and type of vegetation in the same way as in baseline 1 sensitivity analysis, however the percent change in effective shade that results is generally smaller. One reason for this difference is that baseline 2 has a higher starting effective shade than baseline 1, so the percent change in effective shade due to increasing vegetation density is smaller. The temperature response to increased effective shade remains significant within the range tested. As a result the sensitivity coefficient for effective shade indicates high sensitivity. One reason that the temperature response remains significant is the smaller volume of water contained within the banks has a larger temperature response to energy input than the larger volume in baseline 1. The sensitivity of baseline 2 to effective shade is relatively non-linear. The greatest sensitivity occurs with a small increase in effective shade. This result is consistent with the results in baseline 1, where decreasing sensitivity with increasing effective shade was observed. Temperature decreases only slightly more with continued increase in effective shade.

9.5.2.9 Air Temperature and Sediment Sensitivity

As in the first baseline scenario, the sensitivity of this baseline to air temperature is relatively linear. Again in this scenario, the only variable altered was hourly air temperature. The upstream boundary water temperature did not change, as it would have in a realistic scenario. The sensitivity coefficient is smaller, indicating that a watercourse with characteristics described by baseline 2 is not as sensitive to air temperature as the one described by baseline 1. One reason for this decreased sensitivity is that less water surface area is in contact with air than would be for a wider channel. The sensitivity of this baseline to sediment temperature is slightly less sensitive for a similar reason. The channel is not as wide, and conduction is assumed to occur only along the channel bottom. With a narrower channel less water is in contact with the conducting sediment.

9.5.2.10 Incision Depth

For this baseline scenario, there was nearly no temperature response to a change in bank incision. The reason for this may be the presence of dense vegetation at the water's edge as defined by the baseline conditions. With nearly vertical banks, reed canarygrass exists on the banks at the water's edge. Reed canarygrass is more than a meter tall and simulated at 93% density so it casts shadows similar to the shadow from an opaque bank.

9.5.2.11 Sensitivity Analysis Discussion

It is important to realize that a single sensitivity of predicted temperature to effective shade does not indicate the magnitude of temperature change, it indicates the ratio of change in temperature to change in parameter. Because many sensitivities are non-linear, a high sensitivity to an input parameter around one range of values does not necessarily suggest that temperature will have the same relationship to the parameter around other values. The greatest change in temperature for the baseline 2 sensitivity scenarios occurred with a 66% reduction in bottom width but the sensitivity coefficient was not the highest because the large change in bottom width required to obtain this decrease in temperature.

9.5.3 Management Scenarios

To compare the thermal impact of potential management scenarios, this study examined different channel morphologies and riparian vegetation types in order to simulate temperature while keeping discharge constant. The baseline scenario used to evaluate actual agricultural watercourse management alternatives scenarios represents a watercourse designed to be 2 meters in width, with 2:1 side slopes. Channel discharge is approximately 0.5 cfs for all management scenarios. Reed canarygrass vegetation is assumed to occupy only the banks and not obstruct or shade the channel. Based on field observations and proposed maintenance plans, these assumptions represent reasonable parameters for watercourses that have been recently maintained but have not been planted with native riparian vegetation. Under actual field conditions, maintenance activities have been observed to increase groundwater flow and occasionally to access groundwater springs that feed additional cool flow into a channel. While this is a possibility particularly in wet years, the amount of ground water supplied to a channel and the increase in groundwater due to maintenance will be irregular. The cooling impact due to a possible increase in groundwater flow with maintenance should not be considered in the analysis of the impact of maintenance on channel design. Neglecting groundwater flow provides a reasonable worst case scenario and highlights the influence of maintenance design parameters.

Table 9-7 outlines maintenance scenarios considered. Maintenance scenarios are considered in comparison with a baseline condition to determine the relative impact of design options. The predicted maximum seven-day average of daily maximum temperatures is 18.3°C under the baseline condition. Simulation takes place in mid-July using weather data collect in the Puget lowlands in King County during July 2004. Temperatures in the region during July 2004 were considered "Much Above Normal" by the National Oceanic and Atmospheric Administration (NOAA) (http://www.ncdc.noaa.gov/oa/climate/research/2004/jul/currentmonth.html#trD_mo).

Table 9-7. Management scenario results

	Side Slopes	Vegetation	Bottom Width (m)	Flow Velocity (m/sec)	Flow Depth (m)	Effective Shade (0-1)	Max 7-Day Average of Daily Maximum Temperature
Baseline	2:1	RCG	2	0.04	0.15	0.20	18.3
Scenario 1	0:1	RCG	1	0.05	0.28	0.87	18.2
Scenario 2	2:1	None	2	0.04	0.15	0.06	18.4
Scenario 3	0:1	None	1	0.05	0.28	0.31	18.2
Scenario 4	2:1	Willows	2	0.04	0.15	0.90	17.6
Scenario 5	0:1	Willows	1	0.05	0.28	0.99	18.0

9.5.3.1 Management Scenario 1

Refer to Table 9-7 for a summary of the conditions and results of this management scenario. Recall that for this maintenance scenario, water discharge was held constant so as to equal the input used in baseline 1 simulation, but the bottom width was narrowed, the water column deepened, and steeper 0.001:1 side slope. The simulated maximum seven day average of daily maximum temperatures was 18.2°C. By narrowing the channel dimensions and deepening the flow dimensions in this manner, the predicted maximum seven day average temperature decreased by only 0.1°C decrease. Although a temperature decrease of this magnitude indicates slight cooling trend over the length of the reach, it is relatively modest compared to the magnitude of water cooling needed to achieve compliance with Class A or the recent Ecology/USEPA adopted temperature standards for salmonid fish species. Because the flow velocity is slightly higher than that of the baseline, water moving through this system is not exposed to the surroundings as long as it is in the baseline scenario. This gives the environmental thermal balance less influence on water temperature.

9.5.3.2 Management Scenario 2

Refer to Table 9-7 for a summary of the conditions and results of this management scenario. The same input parameters were used as in the listed baseline simulation, however all vegetation is assumed to be cleared. Conditions used in this scenario are similar to conditions that commonly exist following watercourse maintenance and before mitigation plantings begin to flourish. The

predicted maximum seven day average temperature increased by 0.1°C under these conditions. This increase indicated a warmer trend over the reach, albeit a relatively insignificant increase in comparison with the baseline temperature. The velocity of flow and exposure time within this system is the same as that of the baseline, so the influence of the environmental energy balance on has the same potential influence on watercourse temperature as it does in the baseline.

9.5.3.3 Management Scenario 3

Again the reader should refer to Table 9-7 for a summary of the conditions and results of this management scenario. In comparison with Management Scenario 2, this scenario represents the same deeper narrower and faster moving flow assumed in Scenario 1, however, vegetation is assumed to be absent on the banks and in the channel. Under these devegetated conditions, narrowing the channel results in a predicted average daily maximum temperature that is cooler than the baseline predicted average daily maximum temperature. The increase in effective shade in comparison with the baseline scenario is due to bank incision and a narrower water width. This scenario represents conditions similar to many actual watercourses with steep banks following watercourse maintenance. However, it should be noted that deliberate efforts to decrease channel width may not be consistent with U.S. Natural Resource Conservation Service standards that call for a minimum slope angle of 2H:1V for most agricultural drainage channels. Moreover, over steepened stream banks tend to slough saturated soil into the watercourse after floodwaters recede, degrading water quality and depositing sediments on the streambed, thereby potentially decreasing the temporal interval between future channel maintenance operations.

9.5.3.4 Management Scenario 4

Refer to Table 9-7 for a summary of the conditions and results of this management scenario. This scenario simulated the wider, shallower, and slower flowing watercourse simulated in Scenario 1 with the effects of a dense, mature stands of willows on the banks. The highest effective shade considered so far, due primarily to willow trees, combined with the slowest time of travel through the system under this scenario resulted in the largest water temperature impact and the greatest degree of water cooling. The maximum seven day average of daily maximum temperatures predicted in Scenario 4 is 0.7 degrees C cooler than the baseline Scenario. This condition is similar to a watercourse with shallow banks planted with willow vegetation more than two years after maintenance and successful mitigation planting of willows.

9.5.3.5 Management Scenario 5

Refer to Table 9-7 for a summary of the conditions and results of this management scenario. Management Scenario 5 most closely resembles Scenario 1 and produces similar temperature prediction results. Applying willow vegetation to the banks of a narrower, deeper, faster flowing watercourse increases effective shade slightly. With the shorter travel time, the predicted maximum seven day average of daily maximum temperatures is reduced only 0.1°C.

9.6 Conclusions and Recommendations

The goals of this study were to identify the reach scale change in temperature associated with watercourse maintenance and to produce a modeling tool to predict watercourse temperature under different management scenarios. A modified temperature model was developed capable of simulating pre-and post maintenance conditions. These conditions include wetland flow and extensively emergent or overhanging vegetation present before maintenance as well as changes in channel morphology and vegetation due to excavation. The results of this study show that the modified Heat Source 6.0 model predicts diurnal and maximum seven day average of daily maximum temperatures reasonably accurately. Hourly temperature predictions are typically accurate to within less than half a degree. The simulation results can be used to compare downstream watercourse temperature before and after planned maintenance, or to generate predicted temperature data for use in modeling dissolved oxygen. Predicted maximum seven day average of maximum daily temperatures can be used to determine habitat suitability and determine compliance with temperature standards according to EPA's temperature standard guidance before and after planned maintenance.

The modified model can be used to simulate maintenance and mitigation scenarios in order to identify the impact of planned maintenance or to select mitigation and maintenance with the minimum impact. As part of this objective, the model can be used to identify the potential importance and effectiveness of riparian vegetation in protecting watercourse temperature from increase due to maintenance. Sensitivity analysis results and management scenarios show low sensitivity and small temperature response to reach conditions. The small changes observable due to changes within a reach suggest that the upstream temperature boundary condition is a strong controlling factor. Considering the small temperature changes that are observable, sensitivity analysis results show that a steep incised bank increases the effectiveness of vegetation in providing riparian shade, and that shade cast by vegetation and the bank itself can decrease maximum seven day average temperatures by at least 0.7 °C. Several studies site temperature changes of several degrees as a result of changes to riparian vegetation (Brown and Krygier 1970, Chen et al. 1997, Dong et al. 1998, Bartholow 2000b). It is important to consider that greater temperature change that those found in this study may be observed for longer reaches.

Sensitivity scenarios and management scenario results show that shade can play a role in determining the stream energy balance and temperature; however the maximum observed change in temperature was 0.7 °C, while model error was approximately 0.5 °C. The small temperature response indicates the relatively small influence that conditions in a short reach can have on watercourse temperature. Riparian vegetation can have the greatest influence on watercourse temperature for watercourses with vertical side slopes, since vegetation is closest to the water's edge. Willows with significant overhang provide shade to mitigate for the removal of emergent reed canarygrass during maintenance. Sitka willows, Himalayan Blackberry and reed canarygrass were found to be similar in calibrated shade density, ranging from 80% to 100%. The dimensions of Sitka willow after its second year of successful growth make it the most effective in providing short-term shade. The calibrated density for a mature dense stand of Sitka willows was approximately 93%. This calibrated density accurately simulated actual solar radiation measured in the shade of willows spaced one to four feet apart at their base. A shade

calibration was not made for willow stakes in the first summer following fall planting, midway through the first growing season, because effective shade was not present. After two growing season, willows planted on one foot apart were found to have a calibrated density of 80%. Because calibrated vegetation densities did not vary widely among the types of vegetation used in this study, the most important factor determining the effectiveness of vegetation in providing watercourse shade is the amount of shade coverage, and not shade density. The greatest coverage is made possible by tall vegetation with long overhang lengths planted close to the water's edge, such as willows. Of the three vegetation types studied, willows have the greatest potential for providing overhang. If willows trees are grown successfully, willows planted on one bank may be sufficient to shade watercourses of typical size after two successful growing seasons. The model should be applied on a case by case basis to determine the temperature benefit of riparian plantings for a particular watercourse and maintained channel morphology. The absolute change in temperature observed along the length of a reach will depend on reach length, the upstream temperature entering the reach, the time of travel, and the thermal environment within the reach. Each of these factors is considered in the modified model.

Without accurate flow measurements, and information about groundwater exchange, neither field observed nor simulated changes in actual temperature can be attributed to the presence or absence of shade from vegetation. Modeling scenarios that do not consider the potential influence of ground water flow can only provide indicators of the *potential* influence of the factors that they consider. Because the inflow of ground water exhibits interannual variability and also varies by location, it is difficult to consider it using water temperature models developed to assist in planning watercourse maintenance mitigation elements. On the other hand, because ground water will generally have a cooling effect, neglecting this effect provides a reasonable worst case scenario that was likely attained during the validation period in the warm drought years during which validation data was collected.

A single statement regarding the relative importance of shade versus ambient temperature cannot be made for all small agricultural drainage watercourses in King County. The influence and relative importance of various factors will depend on channel morphology at a minimum. Air temperature may be more important in determining the temperature of wide watercourses with sloped banks, while shading vegetation may play a more important role than air temperature for narrower watercourses with vertical banks. Moreover, there are likely other reasons for having stream-side vegetation, such as increased cover, reduced pollutant runoff, and suppression of RCG, which were not including in this temperature study. Nevertheless, our model indicates an overall benefit related to riparian vegetation at least on the bank facing the sun.

In lieu of running the model for every location, it would appear that if the existing stream temperatures in a waterways violate state water quality standards, a prudent "one size fits all" approach would be to require planting of native vegetation along the waterway. The exact type, width, height, and density of plantings are functions of many factors outside the focus of this research. It is imperative for all parties to understand that the relatively short reaches (< 200 m) of many projects means only small improvements in stream temperature. Cumulative impacts along longer waterways may significantly impact some situations but short drainages are unlikely to undergo significant improvement.

Although not specifically considered as a research objective, a question arose regarding the preferred width of riparian shade required to impact stream temperature. This question is not easily addressed since it would require instrumenting numerous field sites with varying widths of shade in order to definitively pick a characteristic width. Brosofske et al. (1997) conducted a study of microclimate impacts of stream buffers surrounding small streams at three western Washington locations. Their investigation examined relative humidity, wind speed, air temperature, solar radiation, soil moisture, and soil temperature. The effectiveness of shade was positive at all widths with soil moisture, soil temperature, and solar radiation at near 100% at widths of one tree height or less on each side of the stream. However, impacts to wind speed and relative humidity required buffer widths of up to 45 m (148 ft) in order to register "no effects." Thus, a considerable range of widths exist depending on the overall final objective.

The Oregon State Department of Environmental Quality (2008), in a temperature study of water quality trading options in the Tualatin River watershed, recommended vegetated corridors ranging from 4.5 to 60 m (15 to 200 ft) on each side of the waterway. For perpendicular slopes less than 25 % (typical of most King County farm areas), recommended widths are shown in Table 9-8. In addition, this study recommended trees (e.g., red alder, western hemlock) be planted at 3 m (10 ft) spacing while shrubs (e.g., red-osier dogwood) be planted at 1.5 m (4-5 ft) distances.

Table 9-8. Stream buffer widths suggested by Oregon

Area definition	Width of vegetated corridor per side
Streams with intermittent flow draining:	
10 to 50 acres	4.5 m (15 ft)
50 to 100 acres	7.6 m (25 ft)
Existing or created wetlands < 0.5 acres	7.6 m (25 ft)
Streams with perennial flow	15 m (50 ft)
Streams with intermittent flow draining > 100 acres	15 m (50 ft)
Existing or created wetlands > 0.5 acres	15 m (50 ft)
Tualatin River	38 m (125 ft)

In summary, given the variability in widths recommended in the literature, our recommendation would be to apply an adaptive management strategy where newly planted vegetation would be monitored over time to see if King County's objectives were being met. As such, we would tend to favor a minimal initial corridor of 2-4 m (5 to 10 ft) coupled with long-term monitoring and evaluation. However, it must be stressed that this recommendation is based solely on literature findings rather than on the science of this investigation.

9.7 References

Amaranthus, A., H. Jubas, and D. Arthur. 1989. Stream shading, summer streamflow and maximum water temperature following intense wildfire in headwater streams. In General Technical Report PSW-109, Proceedings of the Symposium on Fire and Watershed Management, October 26-28 1988, Sacramento, CA. U.S. Dept. of Agriculture, Forest Service. Pacific Southwest Forest and Range Experiment Station, Berkeley, CA.

Baca, R.G. and R.C. Arnett. 1976. A limnological model for eutrophic lakes and impoundments, Battelle Inc., Pacific Northwest Laboratories, Richland, WA.

Beschta, R.L. and R.L. Taylor. 1988. Stream temperature increases and land use in a forested Oregon watershed. Water Resources Bulletin, 24(1), 19-25.

Beschta, R.L. and J. Weatherred. 1984. TEMP-86: A computer model for predicting stream temperatures resulting from the management of streamside vegetation. USDA Forest Service, Report WSDG-AD-00009. Fort Collins, CO.

Beschta, R.L. 1997. Riparian shade and stream temperature: an alternative perspective. Rangelands, 19: 25–28.

Bartholow, J.M. 1989. Stream temperature investigations: field and analytic methods. Biological Report 89(17), US Fish and Wildlife Service, National Ecology Research Center, Fort Collins, CO.

Bartholow, J.M. 1991.A modeling assessment of the thermal regime for an urban sport fishery, Environmental Management, 15 (1991), pp. 833–845.

Bartholow, J.M. 2000a. The stream segment and stream network temperature models: A self-study course. Version 2.0, USGS Biological Resource Division Midcontinent Ecological Science Center, Fort Collins, CO.

Bartholow, J.M. 2000b. Estimating cumulative effects of clearcutting on stream temperatures, Rivers, 7(4), 284-297.

Bartholow, J.M. 2002. Stream segment temperature model (SSTEMP) Version 2.0. Revised August 2002. Fort Collins, CO: U.S. Geological Survey, Fort Collins, CO.

Barton, D.R., W.D. Taylor, and R.M. Biette. 1985. Dimensions of riparian buffer strips required to maintain trout habitat in southern Ontario streams. North American Journal of Fisheries Management, 5, 364-378.

Bicknell, B.R., J.C. Imhoff, J.L. Kittle Jr., A.S. Donigian Jr., and R.C. Johanson. 1997. Hydrological Simulation Program--Fortran, User's manual for version 11: U.S. Environmental Protection Agency, National Exposure Research Laboratory, Athens, Ga., EPA/600/R-97/080, p. 755.

Bormann, M. 2000. The grazier, Oregon State University Extension Service. Vol. 306 no.5.

Bowie, G.L., W.B. Mills, D.B. Porcella, C.L. Cambell, J.R. Pagenkopf, G.L. Rupp, K.M. Johnson, P.W. Chan, and S.A. Gherini. 1985. Rates, constants, and kinetics formulations in surface water quality modeling. EPA/600/3-85/040, Athens, GA.

Boyd, M.S. 1996. Heat Source: stream temperature prediction. Master's Thesis. Departments of Civil and Bioresource Engineering. Oregon State University, Corvallis, Oregon.

Boyd, M.S. and B. Kasper. 2003. Analytical Methods for Dynamic Open Channel Heat and Mass Transfer: Methodology for the Heat Source Model Version 7.0. Oregon Department of Environmental Quality, Portland, OR. Accessed at: http://www.deq.state.or.us/WQ/TMDLs/docs/tools/heatsourcemanual.pdf

Brosofske, K.D., J. Chen, R.J. Naiman, and J.F. Franklin. 1997. Harvesting effects on microclimatic gradients from small streams to uplands in Western Washington. Ecological Applications. 7(4): 1188-1200.

Brown, G.W. 1969. Predicting temperatures of small streams. *Water Resour. Res.* 5(1): 68-75.

Brown, G.W. 1970. Predicting the effect of clearcutting on stream temperature. Journal of Soil and Water Conservation, 25, 11-13.

Brown, G.W. and J.T. Krygier. 1970. Predicting the effects of clearcutting on stream temperature. *Journal of Soil and Water Conservation*. 25: 11-13.

Brown, L.C. and T.O. Barnwell. 1987. The Enhanced Stream Water Quality Models QUAL2E and QUAL2E-UNCAS: Documentation and User Manual. EPA/600/3-87/007, Athens, GA.

Burton, T.M. and G.E. Likens. 1973. The effect of strip cutting on stream temperatures in the Hubbard Brook experimental forest, New Hampshire. Bioscience, (23) 433-435.

Chen, Y.D. 1996. Hydrologic and water quality modeling for aquatic ecosystem protection and restoration in forest watersheds: A case study of stream temperature in the Upper Grande Ronde River, Oregon. Ph.D. dissertation, University of Georgia, Athens, GA. 268 pp.

Chen, Y.D. and H. Chen. (1993). Determining stream temperature changes caused by harvest of riparian vegetation: an overview. Proc. of the Conf. on Riparian Ecosys. in the Humid U.S.: Functions, Values, and Management, Nat. Assoc. of Conservation Dist., Washington, D.C., 281–292.

Chen,Y.D., S.C. McCutcheon, R.F. Carsel, D.J. Norton, and J.P. Craig. 1997. Enhancement and application of HSPF for stream temperature simulation in Upper Grande Ronde Watershed, Oregon.

Chen, Y.D., R.F. Carsel, S.C. McCutcheon, and W.L. Nutter. 1998a. Stream temperature simulation of forested riparian areas: I. Watershed-scale model development. Journal of Environmental Engineering, 124(4), 304-315.

Chen, Y.D., S.C. McCutcheon, D.J. Norton, and W.L. Nutter. 1998b. Stream temperature simulation of forested riparian areas: II. Model application. Journal of Environmental Engineering, 124(4), 316-328.

Crites, R., D. Gunther, A. Kruzic, J. Pelz, and G. Tchobanoglous. 1988. Design Manual: Constructed Wetlands and Aquatic Plant Systems for Municipal Wastewater Treatment. Publication No. EPA/625/1-88/022. Cincinnati, OH: U.S. EPA National Center for Environmental Research.

Crites, R.W. and G. Tchobanoglous. 1998. Small and Decentralized Wastewater Management Systems.McGraw-Hill, New York.

Deliman, P.N., W.J. Pack, and E.J. Nelson. 1999. Integration of the Hydrologic Simulation Program-Fortran (HSPF) watershed water quality model into the watershed modeling system (WMS). Technical Report W-99-2, US Army Corps of Engineers, Engineer Research and Development Center, Washington, DC.

Dong, J., J. Chen, K.D. Brosofske, and R.J. Naiman. 1998. Modeling air temperature gradients across managed small streams in Western Washington. Journal of Environmental Management. 53, 309-321.

Ecology. 2007. "Washington Administrative Code 173-201A-200 Part II-Designated Use and Criteria. Washington State Department of Ecology," Accessed at: http://www.ecy.wa.gov/programs/wq/swqs/criteria-freshwater/wac173201a_200-do.html

Edinger, J.E. and E.M. Buchak. 1979. A hydrodynamic two-dimensional reservoir model: Development and test application to Sutton Reservoir, Elk River, West Virginia. Prepared for US Army Engineering Division, Cincinnati, OH.

Edinger, J.E., D.W. Duttweiler, and J.C. Geyer. 1968. The response of water temperatures to meteorological conditions. Water Resources Research, 4(5), 1137-1143.

Hodgson, S. and T.P. Quinn. 2002. The timing of adult sockeye salmon migration into fresh water: adaptations by populations to prevailing thermal regimes. Canadian Journal of Zoology, 80, 542–555.

Ibqal, M. 1983. An introduction to solar radiation. Academic Press. New York. 213 pp.

Johnson, S.L. 2004. Factors influencing stream temperatures in small streams: substrate effects and a shading experiment. Canadian Journal of Fisheries and Aquatic Sciences, 61(6), 913-923.

Klein, R. 1979. Urbanization and stream quality impairment. Water Resources Bulletin, 15(4), 948-963.

Kopperdahl, F.R., J.W. Burns, and G.E. Smith. 1971. Water quality of some logged and unlogged California streams. Inland Fisheries Administrative Report No. 71-12, California Department of Fish and Game. Accessed at: http://www.fs.fed.us/psw/publications/4351/Kopperdahl.pdf

Larson, L.L. and S.L. Larson. 1996. Riparian shade and stream temperature: A perspective. *Rangelands*. 18(4), 149-152.

Larson, L.L. and P.A. Larson. 1997. The natural heating and cooling of water. *Rangelands*. 19(6), 6-8.

LeBlanc, R.T. and R.D. Brown. 2000. The use of riparian vegetation in stream-temperature modification. The Chartered Institution of Water and Environmental Management, 14, 297-303.

Levno, A. and J. Rothacher. 1967. Increases in maximum stream temperatures after logging in old-growth Douglas-fir watersheds. Research Note PNW-65 Portland, OR. U.S. Department of Agriculture, Forest Service, Pacific Northwest Research Station.

Martin, J.L. and S.C. McCutcheon. 1999. Hydrodynamics and transport for water quality modeling. CRC Press, Boca Raton, FL.

Meehan, W. R., editor. 1991. Influences of forest and rangeland management on salmonid fishes and their habitats. American Fisheries Society Special Publication 19.

Moore, J., J. Miner, and R. Bower. 1999. The effect of shade on water: A tub study. Department of Bioresource Engineering. Oregon State University, Corvallis, OR.

NCDC. 2002. Climate data for Seattle-Tacoma International Airport. National Climatic Data Center. NOAA. Accessed at: http://cdo.ncdc.noaa.gov/ulcd/ULCD

NOAA Fisheries. 2004. Consultation on Remand for Operation of the Columbia River Power System and 19 Bureau of Reclamation Projects in the Columbia Basin. F/NWR/2004/00727

Oke, T.R. 1978. Boundary layer climates. John Wiley & Sons, Inc. New York, NY.

Oregon Department of Fish and Wildlife. 1990. Grande Ronde River sub-basin salmon and steelhead production plan. Portland, OR.

Oregon State Department of Environmental Quality. 2008. Water quality permit program – clean water services NPDES permit. http://www.deq.state.or.us/WQ/wqpermit/cwspermit.htm.

Petersen, B.T., T.K. Stringham, and W.C. Krueger. 1999. The impact of shade on the temperature of running water. Department of Rangeland Resources. Oregon State University, Corvallis, OR.

Poole, G., J. Risley, and M. Hicks. 2001. Spatial and temporal patterns of stream temperature (revised). US Environmental Protection Agency, EPA-910-D-01-003.

Ryan, P.J. and D.R.F. Harleman. 1973. An analytical and experimental study of transient cooling pond behavior. R.M. Parsons Laboratory, MIT, Technical Report No. 161, Boston, MA.

Shepard, D. 2005. Modeling water temperature in small agricultural drainage watercourses. Masters Thesis. Biological Systems Engineering Department. Washington State University, Pullman, WA.

Sullivan, K., J. Tooley, K. Doughty, J.E. Caldwell, and P. Knudsen. 1990. Evaluation of prediction models and characterization of stream temperature regimes in Washington. Timber/Fish/Wildlife Rep. No. TFW-WQ3-90-006. Washington Department of Natural Resources, Olympia, WA, p. 224.

Swift, L.W. and J.B. Messer. 1971. Forest cuttings raise temperatures of small streams in the southern Appalachians. Journal of Soil and Water Conservation, 26(3), 111-116.

Tennessee Valley Authority. 1972. Heat and mass transfer between a water surface and the atmosphere. TVA Water Resources Research Engineering Laboratory, Report 14, Norris, TN.

Theurer, F.D., K.A. Voos, and W.J. Miller. 1984. Instream water temperature model. Instream Flow Information Paper 16. U. S. Fish and Wildlife Service. FWS/OBS-84-15. p. 300.

Thomann, R.V., D.M. Di Toro, R.P. Winfield, and D.J. O'Connor. 1975. Mathematical modeling of phytoplankton in Lake Ontario, Grosse Ile Laboratory, National Environmental Research Center, EPA-660/3-75-005, Grosse Ile, MI.

Tissue, B.M. 2000. Beer-Lambert Law. Accessed at: http://www.chem.vt.edu/chem-ed/spec/beerslaw.html

Wunderlich, W.O. 1972. Heat and mass transfer between a water surface and the atmosphere. Tennesee Valley Authority. Water Resources Research Laboratory Report No. 14. Norris, Tennessee. p. 420.

U.S. Army Corps of Engineers. 1974. Water quality for river-reservoir systems. Technical report, Hydrologic Engineering Center, Davis, CA.

U.S. Army Corps of Engineers. 1997. "Mill Creek Basin, King County, Washington Aquatic Resources Restoration Plan, Seattle, WA.

U.S. Environmental Protection Agency. 2001. Technical synthesis: Scientific issues relating to temperature criteria for salmon, trout, and char native to the Pacific Northwest. Submitted to the Policy Workgroup of the EPA Region 10 Water Temperature Criteria Guidance Project, EPA 910-R-01-007.

US Environmental Protection Agency. 2003. EPA *Region 10 Guidance for Pacific Northwest State and Tribal Temperature Water Quality Standards*. EPA 910-B-03-002. Region 10 Office of Water, Seattle, WA.

US Environmental Protection Agency. 2008. River and stream water quality model (QUAL2K). Accessed at: http://www.epa.gov/athens/wwqtsc/html/qual2k.html

Zwieniecki, M.A., and M. Newton. 1999. Influence of streamside cover and stream features on temperature trends in forested streams of western Oregon. Western Journal of Applied Forestry, 14(2), 106-113.

Appendix 9-A: List of Variables

Channel Dimension Parameters

A_s : Segment surface area (m^2)
WWidth: Water top width (m)
b : Channel bottom width (m)
D : Water depth (m)

Beer-Lambert Law Parameters

A_{0a} : The total opaque area due to the absorbers (m^2)
A : Cross-sectional area (m^2)
I_o : The intensity entering the sample at z = 0
I_z : The intensity entering the infinitesimal slab at z
dI : The intensity absorbed in the slab
I : The intensity of light leaving the sample
σ_A : Cross-sectional area of a molecule represented as an opaque disk (m^2)
F_a : Fraction of photons absorbed
N : Number of molecules per volume

Water Characteristic Parameters

T : Water temperature °C
ρ_{water} : Density of water (kg/m^3)
$c_{p(water)}$: Heat capacity of water (cal/kg-°C)
V : Volume of water (m^3)
ΔT : Change in temperature for a single distance step during the simulation minute (°C)
c_p : Heat capacity of water (cal/kg-°C)
ε_{water} : Emissivity of water (0.95)

Time Parameters

Γ : Day Angle (radians)
JD : Day number of the year (Julian Day)
E_t : The equation of time (minutes)
L_s : Standard longitude (degrees)
L_L : Local longitude (degrees)
L_t : Time correction for longitude (minutes)

Heat Fluxes

Φ: General heat energy flux (cal/m^2-min)
Φ_{solar}: Flux due to shortwave direct and shortwave diffuse solar radiation (cal/m^2-min)
$\Phi_{longwave}$: Flux due to long-wave solar radiation from the atmosphere and riparian vegetation (cal/m^2-min)
$\Phi_{evaporation}$: Flux due to evaporative heat loss (cal/m^2-min)
$\Phi_{convection}$: Flux due convection at the air water interface (cal/m^2-min)
$\Phi_{streambed}$: Flux due to conduction between the water column and stream bed (cal/m^2-min)
Φ_{SRC}: Extra terrestrial solar constant (cal/m^2-min)
Φ_{SRE}: Flux from direct solar radiation at the earth's outer atmosphere (cal/m^2-min)
Φ_{SRA}: Flux from direct beam solar radiation routed through the atmosphere (cal/m^2-min)
Φ_{total}: Total heat flux (cal/m^2-min)

Earth Sun Physical Relationship Parameters

r : Ratio of the earth to sun distance, to average earth to sun distance (dimensionless)
$Trans_{atm}$: Transmissivity of the atmosphere (dimensionless)
θ_{sun} : Solar altitude (radians)
θ_{LAT} : Latitude (radians)
τ : Angular rotation of time (radians)
M : Optical air mass thickness (m)
Elevation: site elevation above sea level (m)

Vegetation Parameters

λ : Riparian extinction Coefficient (m^{-1})
VegDensity: Density of riparian vegetation (dimensionless)
$VegH_{actual}$: Height of riparian vegetation (m)
Veg_{width}: Width of vegetation from bankfull edge perpendicular to the bank (m)
PL_{veg} : Approximated path length of solar radiation through riparian vegetation (m)
$Transverse_0$: Distance from the water's edge to the bankfull mark (m)

Bed Conduction Parameters

σ : Stefan-Boltzmann constant (1.83 x 10^{-11} cal/cm^2-min)

ρ_{bed} : Volumetric weighted density (kg/m^3)

$\rho_{seidment}$: Substrate density 1600 (kg/m^3)

α_{water} : Water volume ratio (dimensionless)

$\alpha_{sediment}$: Sediment volume ratio (dimensionless)

$D_{sediment}$: Depth of conduction layer (m)

K_{water} : Water thermal conductivity 0.60 (J/ m s °C)

$K_{sediment}$: Sediment thermal conductivity 15.98 (J/ m s °C)

K_{bed} : Volumetric composite thermal conductivity in conduction layer (J/ m s °C)

ν_{water} : Water volume in conduction layer (m^3)

$\nu_{sediment}$: Substrate volume in conduction layer (m^3)

$\nu_{Hyporeic}$: Total volume in conduction layer (m^3)

$\vartheta_{sediment}$: Porosity of the conduction layer (dimensionless)

$\Psi_{sediment}$: Substrate thermal diffusivity (m^2/s)

Ψ_{water} : Water thermal diffusivity (m^2/s)